Response of full-scale piles to EPBM tunnelling in London Clay

Selemetas D. and Standing J.R.

Abstract The installation and working test performance of four full-scale instrumented driven piles and their subsequent response to twin tunnels constructed below the pile bases are described. One pair was designed to be largely friction piles and the other pair end-bearing. Their locations relative to the new tunnels were carefully chosen to optimise the understanding of pile response at varying offsets from the centre-lines. The site conditions and the greenfield response to EPBM tunnelling at the site were described in a companion paper that reported an expanding displacement field around the tunnels compared with contracting fields usually observed. Field monitoring results indicate that, during construction, zones of influence exist around tunnels (similar to those proposed by Kaalberg et al., 1999 and Jacobsz et al., 2001), where the ground and piles are subjected to different degrees and senses of relative vertical displacement. Redistributions of load along the pile lengths occur as the tunnel boring machines approach, pass beneath and continue beyond the pile bases and lateral pile deflections and bending moments are also induced. Based on the results from this field study, implications for the capacity of existing piles (and design of new piles) subjected to tunnelling-induced movements are assessed for cases of expanding and contracting displacement fields.

Keywords: Tunnelling, piles, soil-structure interaction, field instrumentation and monitoring

Introduction

The subject of tunnelling near piled foundations has received particular attention during construction planning of London's Jubilee Line Extension (JLE), Amsterdam's North/South Line, the Channel Tunnel Rail Link (CTRL) and more recently Crossrail in London. There is a scarcity of well-documented field studies on this subject. Two notable exceptions include the Heinenoord full-scale trial near Rotterdam (Kaalberg et al. 1999) and the study by Coutts and Wang (2000), which presents field results from instrumented piles subjected to tunnelling-induced movements, as part of the North-East Line Project in Singapore (see also Pang et al., 2006). In the Heinenoord study the response of 38 timber piles and 18 concrete piles was monitored during construction of 8.3-m diameter twin tunnels through both Holocene deposits (layers of soft clay and peat) and Pleistocene dense sand. These field observations indicated that pile settlements can be grouped into three categories, depending on the position of the pile toe relative to the tunnel axis (Kaalberg et al. 1999). Jacobsz et al. (2001, 2004) describe the results from a number of centrifuge model tests investigating the form of these zones of influence for the case of tunnelling near axially loaded piles driven in dry sand. Similar zones

of influence in which pile settlements could be correlated with surface movements were identified from these tests. Other noteworthy model studies include the work of Bezuijen and Van der Schrier (1994) and Loganathan et al. (2000). The subject has also been studied numerically (Vermeer and Bonnier, 1991; Mroueh and Shahrour, 2002), as well as analytically (Chen et al., 1999).

The research described in this paper was instigated following assessments of piled structures affected by tunnelling works encountered during construction of the JLE (Geilen and Taylor, 2001a & b, Selemetas et al., 2002) and the studies by Kaalberg et al. (1999) and Jacobsz et al. (2001, 2004). Planned construction of the CTRL presented an opportunity to install four full-scale instrumented piles and monitor their response to tunnelling. Details of the site chosen, the ground conditions, tunnelling operations and the greenfield ground response to tunnelling with an Earth Pressure Balance Machine (EPBM) Tunnel Boring Machine (TBM) are given by Standing and Selemetas (2013). Few comprehensive records of the greenfield ground response to EPBM tunnelling in London Clay exist and so this formed an essential component of the study.

Field research piles

Pile layout

The four instrumented piles were driven-cast-in-situ with a nominal diameter of 480mm. Two of the piles were end-bearing (BC and BO) in the Terrace Gravels with a total length of 8.5m, while the other two (referred to as friction piles, FC and FO) were 13m in length and founded in London Clay. Figure 1 shows the positions of the pairs of end-bearing and friction piles, relative to the two tunnels and the soil stratigraphy. Piles BC and FC were installed directly above the Up-Line tunnel centre-line and piles BO and FO at an offset of 9m from it. These pile locations were strategically selected to investigate the existence of zones of influence established by Kaalberg et al. (1999) and Jacobsz et al. (2001).

Pile instrumentation

The piles were instrumented with: vibrating-wire strain gauges to monitor strains and hence obtain the load distribution along the pile; base load cells to provide an independent measure of the load at the base of the piles; and electrolevel inclinometers for deriving the deflection profile of the piles (see Figure 2).

Clusters of four Gage Technique embedment concrete strain gauges, placed at 2 m intervals along the pile lengths, were attached but not integrally connected to the reinforcing cages of the piles. These devices had a resolution of 1 με and range of 3000 με. One of the strain

gauges at each level was also equipped with a thermistor to record temperature changes. Four strain gauges were used (i) to obtain a good average output and (ii) in orthogonal pairs, in line and perpendicular to the TBM drives, to assess bending moments along the pile lengths.

The base load cells adopted, developed at the Building Research Establishment (BRE), are described in detail by Price and Wardle (1983). The load cells consisted of three 600-kN capacity units for each of the end-bearing piles (BC and BO) and four 280 kN units for the friction piles (FC and FO) and had a resolution of about ±1 kN. The load cells were attached to the bottom of the pile reinforcing cages and each was equipped with a peripheral rubber tube which, once inflated, provided a seal around the cell and a separation boundary, to ensure that the entire axial load on the base would pass through the cell unit. Pressure was maintained in the tube, following cage installation, until the pile grout had set.

Inclinometer casings were attached to the reinforcing cages, with the keyways orientated in the same sense as the strain gauge pairs, i.e. in line with and perpendicular to the TBM drives. After pile construction, pairs of electrolevel devices were installed at 2 m spacings within the inclinometer casing grouted into the pile: their operation and interpretation being the same as those used for monitoring horizontal ground displacements. The level of each pair of electrolevels corresponded to that of the strain gauges. The electrolevel inclinometers, as well as allowing profiles of tunnelling-induced pile deflections to be determined, also allow bending moments along the pile length to be calculated and corroborated with the strain gauge data.

The displacement of each pile relative to the ground surface was monitored by means of four potentiometric displacement transducers (PDTs) set up at the head of each pile. Two pairs of PDTs were each mounted on a reference beam (one either side of the pile head) supported each end on stakes driven a minimum of five pile diameters from each pile, which is greater than the minimum distances recommended in the latest ICE Specification for Piling and Embedded Retaining Walls (ICE, 2017). Changes in the absolute level of the reference beams were monitored by precise levelling onto bar-coded strips that were permanently attached to the stakes. Thus each pile had four bar-coded strips (at both ends of the two reference beams) which were monitored by a dedicated, permanently set up, precise level for greater stability, accuracy and frequency of measurements. Absolute and relative pile head and ground vertical displacements were determined from this system. Readings from this specific exercise were integrated into the precise levelling runs for the ground monitoring, relating them to the same datum point, on a piled structure about 60 m from the research site, as described by Standing and Selemetas (2013).

Pile installation

The research piles were driven-cast-in-situ, constructed by top-driving a steel tube fitted with an expendable steel shoe to the required depth using a Junttan PM25 piling rig. The steel tube had an external diameter of 456mm and wall thickness of 20 mm while the bottom steel shoe was 500 mm in diameter. The original intention was to place the reinforcing cage, with attached instrumentation, inside the tube after driving and then carefully tremmie in the grout to avoid any damage to the instruments, prior to extracting the tube. However, due to limited clearance between the base load cells and the inner wall of the piling tube, this was not possible and so the reinforcement cage with the instrumentation was inserted following the removal of the steel tube, similar to a conventional continuous flight auger CFA pile. In the case of pile FC it was not possible to install the reinforcing cage to the required depth, as the grout was setting and too thick to flow around the base load cell. Consequently the base load cell in this pile only reached 10.3 m, rather than the planned depth of 13 m.

The pile reinforcement cage consisted of eight B20 bars with shear links of B8 bars spaced at 300 mm. Additional short lengths of B8 bars were welded between adjacent B20 bars to provide support for the vibrating wire strain gauges (see Figure 2). The grout used for the piles had a 1:1 sand to cement ratio. Samples of grout taken from piles BC and FC gave average compressive cube strengths of 53.3 and 50.5 MPa respectively.

Pile response during initial loading

One month prior to the arrival of the first, Up-Line, EBPM TBM all four piles were loaded to approximately 50% of their estimated ultimate capacity using kentledge reaction platforms. Loads were maintained using load cells to within about ±0.5kN, prior to and during tunnel construction using an automatic computer-controlled system with compressors supplying pressure to air-oil interfaces linked to hydraulic jacks. Each of the end-bearing and friction piles was loaded with 650 kN and 240 kN respectively.

Pile loading involved applying incremental axial head loads (P) with each load increment maintained for a one-hour period. Applied loads and corresponding pile head displacements (S_p) were recorded at five-minute intervals. Results for the four piles during loading are given in Table 1 (values of pile settlement represent final values at the end of each load increment, while load values correspond to average values over each increment). This procedure was to simulate a pile load test in order to obtain load-displacement curves and to estimate pile capacity in terms of shaft capacity and end-bearing.

Pile load-displacement curves for the friction and end-bearing piles are shown in Figure 3, where they are compared with analyses using the CemSet method developed by Fleming (1992). The CemSet parameters used to re-produce the pile test response are summarised in Table 2. The load-displacement responses of the friction piles are remarkably similar, albeit the loading range covered is limited. At the end of the final load increment the total pile settlement was less than 1 mm for both piles. In comparison the two end-bearing piles show slightly different responses with pile BC having a stiffer load-settlement relationship. Total pile settlements were 4.6 mm for Pile BO and 3.8 mm for pile BC. The final values of pile settlement indicate that the friction piles FC and FO mobilised a small portion of their total shaft friction along their lengths while the end-bearing piles BC and BO mobilized their full shaft friction during the pile test. The stiffer response of pile BC can be attributed to the presence of denser Terrace Gravels below the base of this pile. Tube driving records during pile installation, in the form of number of blows per 0.25 m versus depth, indicate that this stratum is denser at the positions of piles BC and FC compared with the locations of piles BO and FO (Selemetas, 2005).

Pile stiffness and load distribution with depth

Distributions of axial load along the pile lengths are determined indirectly from measurements of strain. The measured strain at each pile level is multiplied by the pile cross-sectional area and the pile stiffness to obtain the resulting axial load at this level. Pile stiffness, E_p, is calculated from the ratio of applied stress over average strain measured near the top of each pile. As the level of the upper strain gauges is very close to the ground surface (<0.25 m for piles FO, BO and BC), pile shaft friction should be negligible and the load acting at this level is assumed to be equal to the applied load at the head of each pile. This is not the case for pile FC with strain gauges at 1.5 m below ground surface.

The development of back-calculated pile stiffness for piles FO, BO and BC with time starting from immediately after the end of the final pile loading stage is shown in Figure 4a. The stiffness of pile FC is assumed to be equal to that of pile FO. The stiffness of the three piles follows the form of an exponential function with a maximum value of $E_{p\,(max)}$ = 23.4 GPa one day after the final pile loading stage, reducing to approximately 75% of $E_{p\,(max)}$ over the next 68 days (Figure 4b). The power curve presented in Figure 4b is a normalized best fit curve for the three back-calculated curves shown in Figure 4a following a regression analysis. The reduction of pile stiffness with time is due to time-dependant creep strains that occur in each pile. The maximum back-calculated value ($E_{p\,(max)}$) agrees well with values that would be obtained from code recommendations and best industry practice documents by making an allowance for creep effects, e.g. BS EN 1992-1-1 (BSI, 2004).

The load transfers along the four piles at the end of each loading stage, assuming zero strain at the onset of loading (i.e. no initial residual strains), are shown in Figure 5. During pile loading, a significant amount of shaft resistance was mobilized for all piles within the made-ground, i.e. within the first 3 m of depth, while little or no shaft friction was generated in the alluvium. This is particularly evident in pile BC for which the axial strains at levels below –3 m are almost identical indicating that little or no shaft friction is mobilized along the length of the pile in the alluvium, which extends to 7.5 to 8 m. Friction piles FC and FO transferred most of their load through shaft friction, with pile FO carrying only 10% of the applied load in end-bearing. Pile BO also exhibits significant shaft friction take-up, carrying only 40% of the final applied load at its base. In comparison, pile BC behaves more like an end-bearing pile, carrying about 60% of the total applied load in end-bearing. The almost parallel load-transfer profiles in Figure 5 indicate that the shorter piles BC and BO have mobilized their shaft capacity during pile loading, unlike the longer friction piles which have some reserve shaft capacity.

Prior to loading, the piles were subjected to unintentional ‘pre-loading’ effects from the initial placement of kentledge on the ground (i.e. before its load was transferred to the piles). Surface settlements from this temporary kentledge load are presented and discussed by Standing and Selemetas (2013). Following the installation of the driven pile, negative shaft friction develops along the length of the pile where the consolidating soil is moving down relative to the pile, giving rise to a locked-in ‘residual’ load (see Fellenius 2004). If we consider that there is no residual load in the pile and we monitor the load induced in the pile during static pile testing, this load distribution is referred to as ‘apparent’ load. The ‘actual’ load distribution is simply the superposition of the ‘residual’ and the ‘apparent’ load distributions. The residual loads measured in the four piles prior to loading, are presented in Figure 6 along with the apparent axial load distribution after pile loading (ignoring any residual load), and the actual load distribution in the piles obtained by superimposing the curves of residual and apparent load. The apparent axial load distributions are identical to the final load transfer curves shown in Figure 5. The actual load distribution curves at the end of pile loading describe a more gradual transfer of load from the top of each pile to its base. Failure to account for residual loads generated in the piles would result in an overestimation of pile shaft friction and an underestimation of pile base load.

Pile response to tunnelling

Pile settlement due to tunnelling

In reviewing the tunnelling-induced pile settlements, it is useful to compare tunnelling-induced pile head displacements with those of the surrounding ground surface. Emphasis is placed on the ratio of absolute pile head displacement, S_p, to the surrounding ground surface vertical displacement, S_g, which is denoted as R (i.e. $R = S_p/S_g$). Thus, R values greater than unity indicate that the pile head has settled more than the ground surface giving rise to Differential Pile Settlement (where $DPS = S_g - S_p$, a negative value). Conversely R values less than unity imply Differential Pile Heave ($DPH = S_g - S_p$, a positive value) relative to the ground.

Up-Line tunnel – pile vertical displacements

Variations in applied load at the head of pile FC (above the centre-line of the Up-Line tunnel) with time and the development of pile vertical displacement with time compared with the corresponding ground movements during construction of the Up-Line tunnel are shown in Figures 7i: a and b. Also plotted is the advancement rate of the TBM showing the position of the EPBM face relative to pile FC. Standing and Selemetas (2013) describe and link the ground response to the approach and passing of the TBM. During the passage of the EPBM, the applied load at the head of the pile exhibits small variations due to thermal effects and sensitivity to pile movements: maximum changes were less than 20 kN. Initially the ground and pile heave by about 2 mm as the face approaches, resulting in small pile load increases. Immediately after the EPBM face passes underneath the pile, both the pile and the ground settle, with the pile settling more than the ground (S_p = 4.0 mm; S_g = 1.7mm), i.e. $R > 1$, resulting in the pile load reducing (at about 38 days). A small degree of further heave then occurs from tail-skin grouting. Following the passage of the shield and the tail grouting phase, both the pile and the ground show small sudden settlement (at about 42 days) when the TBM started again (after delay of 41 hours as it was necessary to rebuild a damaged ring) followed by gradual tunnelling-induced consolidation (about 4 mm over the course of 23 days).

Construction of the Up-Line tunnel did not significantly influence pile FO (at 9m offset from its centre-line), as shown in Figures 7ii: a and b. The pile follows the pattern of ground surface displacement during and following the passage of the Up-Line TBM, i.e. R=1 for most practical purposes. Magnitudes of initial heave and final settlement for pile FO were less than those of pile FC. Reasons for the applied pile load increasing to approximately 260 kN (from the target control value of 240 kN) are not known.

End-bearing pile, BC, experienced a similar response to the centre-line friction pile FC (Figures 7iii: a and b). Initially the pile heaved by 0.5 mm with the arrival of the EPBM face

(smaller heave than of pile FC because of the greater distance between pile toe and tunnel crown, 6.35 m versus 1.85 m). The pile BC toe level is just within the zone of ground heave reported by Standing and Selemetas (2013). During this initial heave the load applied at the top of pile BC increased rapidly from 660 kN to about 700 kN. The applied load was quickly restored to its target value of 650 kN, but continued to show high sensitivity during the passage of the EPBM face beneath the pile. The 41-hour delay of the EPBM occurred when its face was almost directly beneath pile BC (which is 18 m from pile FC – see Figure 1). During this period the ground and the pile settled gently but once the EPBM started progressing again the rate of pile settlement accelerated rapidly and the applied load at the top of the pile suddenly increased to 750 kN. At this time, pile BC settled more than pile FC at the same stage (6.5 mm versus 4 mm), because of much greater load acting on it. The applied load was quickly restored to its original value but subsequently increased rapidly to 800 kN again during tail-skin grouting. With time the pile and the ground continue to settle due to consolidation, reaching values of S_p = 10 mm and S_g = 7mm 20 days after the passage of the shield beneath the pile. The sudden heave shown by pile BC on day 49 (Figure 7iii: b) corresponds to a temporary reduction in the load at the top of the pile (Figure 7iii: a).

The response of offset pile BO (9 m from Up-Line tunnel centre-line) is similar to that of FO (Figures 7iv: a and b), with greatly reduced displacements and very small load changes. Pile BO and the surrounding ground experience slight heave followed by gradual settlement after the passage of the TBM, with the R values being equal to 1. The applied load on pile BO was well controlled during tunnel construction and there were no signs of influence from the events causing construction delays.

Down-Line tunnel – pile vertical displacements

Incremental vertical displacements and applied loads for the friction and end bearing piles during passage of the Down-Line tunnel are shown in Figure 8. Piles FO and BO are now at an offset of 7 m from the centre-line of the Down-Line tunnel (which is a similar offset to that from the Up-Line tunnel, c.f. 7 m with 9 m), while piles FC and BC are at an offset of 16 m. The response of piles FO and BO is almost identical to that of the surrounding ground during and following the passage of the Down-Line EPBM. This correlates well with their response to the Up-Line tunnel construction for which they were at a similar offset. Both piles show a short-term settlement of approximately 5 mm (Figure 8ii:b and iv:b), with negligible initial heave, followed by consolidation settlement of 5 mm over a period of 10 days. In comparison, piles FC and BC, at a greater offset, experience negligible or only slight settlement due to tunnelling. Consolidation settlements of the ground surrounding them were slightly greater, imposing a small degree of negative shaft friction on these piles.

Differential pile displacements

Pile head displacements in the form of differential pile displacements (DPS and DPH) against distance from the face of the tunnelling shield are presented in Figure 9 for the Up-Line TBM drive. The piles show clear trends in behaviour during the various construction phases. Pile FC initially experienced slight differential heave with the TBM face about 4 m away ($y = -4$ m) followed by differential settlement just before the TBM face passed beneath the pile. This initial heave is hardly surprising in view of the clearance of only 1.9 m between the pile toe and the tunnel crown and the high EPB pressures applied at the face of the excavation. Pile BC, with a clearance of 6.4 m from the tunnel crown, exhibited no differential heave and only slight differential settlement at a distance of about $y = -2$ m from the TBM face. These responses indicate that EPBM tunnelling is very efficient in minimising the differential displacements ahead of the face but once the TBM face is directly beneath the piles a sudden increase occurs.

As the TBM face progressed beyond piles FC and BC, they settled more than the ground, over a distance of up to 10 m, corresponding to the length of the EPBM shield. Measurements from the pile instrumentation indicate that during this stage both piles experience a reduction in their base load which is compensated by a mobilisation of reserve shaft capacity, hence resulting in differential pile settlement relative to the ground. In particular, Pile FC (of length of 13m) experiences 2.5 mm of differential pile settlement compared with 4mm for pile BC (of length 8.5 m). The difference can be partly attributed to the different loads applied to each pile and the difference in pile lengths (a longer pile settling less than a shorter pile to mobilise the same amount of shaft capacity). The results suggest that this phase, when the shield passes beneath the pile, is the most critical in terms of the impact on adjacent structures, as it causes the greatest differential displacements.

Tail-skin grouting takes place following the passage of the shield to fill the void between the most recently placed segmental ring and the ground. This causes slight differential heave of about 0.5mm for piles FC and BC (at just beyond $y = 10$ m). Subsequently, the piles experience small differential settlements, the rate of which rapidly diminishes.

During construction of the Down-line tunnel piles FO and BO (at an offset of 7 m from the tunnel centre-line) experienced negligible differential pile settlement, i.e. $R \sim 1$. In the case of piles FC and BC (at an offset of 16 m) the surrounding ground settled slightly more than the piles (i.e. differential pile heave with $R<1$) implying that negative shaft friction is induced along the length of these piles.

Axial load response due to tunnelling

Axial loads within the piles are discussed using the values determined from the strain gauge clusters positioned along their lengths. Near the base of each pile, the pattern of axial load *change* measured from the strain gauge readings was of similar form to that from the base load cell measurements. However, in most cases, the absolute magnitudes of loads registered from the base load cells were less than those determined from the strain gauge clusters. This is thought to be caused from the peripheral rubber tube around the base load cell not expanding fully during installation and grouting, resulting in some load by-passing the base load cell unit. Base load cell results are therefore not presented.

Up-Line tunnel – pile load distributions

Axial loads for each strain gauge cluster position along the length of pile FC during construction of the Up-Line tunnel are plotted versus time in Figures 10a to f; the distance of the EPBM face from the pile is also shown. The load plotted at a depth of z = 0 m (Figure 10a) corresponds to the applied load at the top of the pile, which remained reasonably constant at 240 kN. Prior to the TBM influencing the pile, this load applied at the top of the pile can be seen to reduce with depth (i.e. at each cluster point), as it is distributed to the ground via shaft friction. Key points during tunnel construction can be identified for each of the traces (O, A, B, C and D): they are only marked on Figure 10d. Point O represents the initial load prior to tunnel construction. The face and rear of the EPBM are directly beneath the pile at points A and B respectively. Point C denotes the end of tail-grouting and point D corresponds to the final load after tunnel construction.

As the TBM approaches pile FC the axial compressive load starts to increase gradually at all levels from the EPBM face pressure, with a maximum increase of 120 kN at a pile depth of z = −5.5 m (i.e. around the midpoint of the pile length), when the face is directly beneath the pile (point A). Loads then reduce as the EPBM shield passes beneath the pile which is settling more than the ground over this duration (see Figures 8 and 10). Axial loads remain constant during the 9-hour interruption to tunnelling at y = 2.4 m but on recommencement decrease slightly further until the rear of the EPBM passes beneath the pile (point B, y = 10 m). Tail-skin grouting, just after this time, causes another increase in the axial load (point C). A gradual reduction in loads (except at the head of the pile) occurs during the 41–hour delay period when the EPBM was stationary at y = 17 m. After another small increase in load, once tunnelling begins again, there is a gradual reduction in the axial load with time until steady values are reached after about y = 30 m (point D).

Reduction in loads before and after tunnel construction are evident at all levels beneath the ground surface, with maximum net changes of about −100kN over the middle length of the pile (e.g. z = −5.5 m and −7.5 m; Figures 10d and e). Subsurface measurements broadly corroborate this observation as discussed below. Overall changes in the axial loads with distance along pile FC at times corresponding to the key events of the Up-Line tunnel construction are summarized in Figure 11a. Curve O shows the initial load distribution prior to tunnelling with the reduction in load with depth as the 240 kN applied at the head is distributed to the ground via shaft friction (c.f. actual load in Figure 6a).

The effects of the stages of TBM progress and tunnel construction are now described and discussed in terms of pile loads and vertical displacements of the ground (surface and subsurface) and pile head (with reference to Figures 10 and 11a).

(i) The arrival of the EPBM face beneath the pile (point A, at y = 0) induces an axial compressive load of increased magnitude near the middle of the pile. This can be explained under two contexts. First, there is a small differential pile heave at the surface (<1 mm relative to the ground, Figures 7ib and 9a), implying that the base of the pile is being pushed upwards (by the face pressure) more than the ground. Secondly, at the same time, the ground surface heaves by 1−2 mm (Figure 7ib), while the ground just above the tunnel (at z = −14 m) heaves by about 5 mm (Standing and Selemetas, 2013). Compressive ground strains and stresses generated by these relative displacements would be transmitted to the pile at the ground–shaft interface.

(ii) During the passage of the shield beneath the pile (A−B), pile loads reduce very significantly, the final distribution at B indicating a progressive reduction with depth (Figure 11a). This corresponds to when the greatest differential pile settlement at the surface is generated (from about y = 0 to 4 m, Figures 7ib and 9a), the pile moving down about 2 mm more than the ground. Downward displacement of the pile would halt if greater shaft resistance were mobilised along its length. The relative vertical ground displacements generated up to point A, increase markedly as the TBM progresses further (to B). In the made-ground and alluvium there are uniform settlements of about 1 mm (i.e. negligible vertical strains in these two strata) while just above the tunnel crown (at z = −14 m) the ground heaves by a further 10 mm as discussed by Standing and Selemetas (2013). Vertical and lateral ground stresses would increase from the compressive strains induced within it (within the Terrace Gravels and London Clay). As a result radial stresses on the pile shaft, σ_r', would increase thus providing greater shaft capacity (assuming a simple relationship of shaft friction = $\sigma_r' \tan \delta'$, with δ' being a constant angle of interface shearing resistance). It is postulated that

the increased shaft capacity from this effect would mean that greater amounts of shaft friction can be mobilised, thus progressively reducing pile loads with depth along the pile.
(iii) Tail-skin grouting behind the shield (point C) induces increases in loads along the length of the pile which can be attributed to similar reasons for those observed from the effects of the face pressure as the TBM approached the pile. By coincidence, the resulting absolute load distribution at this point is almost identical to the original distribution prior to tunnelling.
(iv) The axial load along the pile reduces with time to a steady value (point D), from stress increases from the rapid consolidation that occurred after tunnel construction (Standing and Selemetas, 2013).

Incremental changes in load along the pile length between certain key stages are shown in Figure 11b. The final net change in the axial load during tunnel construction (path O − D) is negative in magnitude, i.e. a reduction in load is induced in the pile due to tunnel construction with a maximum value of 100 kN over the central length of the pile. As the load at the head of the pile remains constant, this reduction results from a combination of differential ground-pile displacements and increased stresses around the pile, allowing greater shaft capacity to be mobilised.

Offset pile FO, 9 m from the Up-Line centre-line, initially experienced a very small reduction in the axial load as the EPBM face approaches the pile (< 10 kN), followed by increases in axial load of up to about 50 kN from consolidation of the ground around the pile at this offset. Profiles of load distribution along the length of the pile before and well after passage of the TBM are shown in Figure 12.

The response of pile BC is broadly similar to that of pile FC in that the axial load initially increases as the EPBM face approaches the pile and then reduces in magnitude as the shield passes beneath the pile before the base load rises up again due to tail grouting. However, significant variations in the load applied at the top of the pile (due to poor control during differential settlement and tail-grouting) clearly influenced the axial load response of pile BC.

During the passage of the EPBM shield beneath the pile, the rate of advance of the tunnelling shield is also shown to influence the axial load distribution along the pile. When the EPBM face is beneath or a few metres beyond the pile, the axial load is shown to remain constant during a pause in EPBM advance. This is followed by a short abrupt increase in the axial load once tunnelling commences again.

Down-Line tunnel – pile load distributions

During the Down-Line tunnel construction the changes in the axial load of all piles were small. Piles FO and BO (at an offset of 7m from the Down-Line tunnel centre-line) showed a small reduction followed by a gradual increase in the axial load bringing the load distribution to values slightly higher than the original. Piles FC and BC (at an offset of 16 m from the Down-Line tunnel centre-line) showed a very slight gradual increase in their axial loads with time due to negative shaft friction, induced by soil movement. This negative shaft friction and subsequent increase in the pile base load with time was slightly larger in magnitude in the case of the longer friction piles FC and FO, as might be expected.

Pile bending moments and deflections due to tunnelling

Tunnel construction induced small bending moments along the piles in the transverse direction to tunnelling and transiently in the direction of tunnelling. The maximum magnitude of bending moment measured in pile FO was just over 20 kNm at a depth of 8 m, which corresponds to about 15% of the ultimate bending capacity of the pile without axial load. In view of the small magnitude of bending moments observed, they are not discussed further here, specific details are provided by Selemetas (2005). In cases where the piles are founded below the invert of the tunnel, it is expected that the bending moments induced would be significantly greater and, if the proposed tunnelling works were known of in advance, would govern the reinforcement design for these piles.

Implications for design practice

Prediction of pile settlement to tunnelling

From the results of this study it is evident that zones develop around an EPBM when tunnelling in London Clay, similar to those presented in previous studies (e.g. Kaalberg et al. 1999 and Jacobsz et al. 2001), in which pile head and ground surface settlements can be correlated. In summary and as shown in Figure 13, piles with their bases located in Zone A settled 2-4 mm more than the ground surface ($R>1$). Piles with their bases in Zone B (defined by a line inclined at 45º between zones A and C) settled by the same amount as the surface ($R=1$), while piles with their bases in Zone C were found to settle less than the surface ($R<1$). Therefore for most practical applications reasonable predictions of pile settlement could be made by using the Gaussian curve as a reference frame. The critical zone is zone A in which piles are likely to settle more than the ground. This additional settlement is likely to be in the range of 2-4 mm (see Figure 9) for volume loss values less than 0.5% (as was the case at the research site, described by Standing and Selemetas, 2013). In general the additional settlement would depend on the following factors: the operation of the EPBM shield: the reduction in the pile

base load; the available reserve shaft capacity along the length of the pile; the pile diameter, the soil type and the volume loss.

Pile design for piles subjected to tunnelling-induced movements

A simple assessment of the effects of tunnelling induced movements on the load distribution in a pile can be made by using the framework of Fellenius (1988) and the CemSet method by Fleming (1992). Figure 14 shows the key load changes for pile FC as presented in Figure 11b (when the EPBM face is beneath the pile and post tunnelling) compared with the envelope of theoretical ultimate shaft friction (USF) along the length of the pile, as back-calculated from the CemSet analysis carried out after the pile loading test. The theoretical shaft friction is plotted both from the head of the pile to the pile toe and from the toe of the pile to the head of the pile, which allows the neutral axis of the pile to be identified at a depth of 9 m. Also plotted is the mobilised axial load in the pile, Q_t, which can be deduced as a function of the relative soil to pile movement for the expanding and contracting displacement fields described in Standing and Selemetas (2013). The mobilised pile load, Q_t, can be expressed as a function of the shaft stress, q_s, with depth, z, in the pile using the following expression:

$$Q_t = \frac{\delta_{mob}}{\delta_{limit}} \pi D \int_0^L q_s dz \qquad \text{[Eq. 1]}$$

where D is the pile diameter, δ_{mob} is the soil displacement at the pile interface (relative to the pile toe) mobilising positive or negative shaft friction and δ_{limit} is taken as 6 mm for friction piles (this being a value commonly adopted in practice for piles in clay). Fleming et al. (2009) quote that this value typically varies between 0.5% and 2% of the pile diameter for piles in clay. The designer can use equation 1 to predict the likely compressive and tensile loads induced in the pile, as a function of the anticipated displacement fields due to tunnelling. Where there is additional compression, the designer should ensure that the allowable compressive stress in the concrete is not exceeded under serviceability conditions and where there is tensile stress induced, the designer must check that piles are reinforced to the right level, if net tension occurs. From a serviceability perspective, tunnelling-induced pile settlements in friction piles can be adequately controlled by designing piles to have reserve shaft capacity, as was demonstrated by the response of pile FC in this case study.

Conclusions

Three zones of influence were identified around the EPBM tunnels in London Clay, similar to those presented in previous studies (see Kaalberg et al. 1999 and Jacobsz et al. 2001), in which pile head S_p and ground surface settlements S_g can be correlated using $R = S_p / S_g$. Piles with

their bases in Zone A were shown to settle 2-4mm more than the ground surface (R > 1). Piles with their bases in Zone B (defined by an angle of 45 degrees between zones A and C) settled by the same amount as the surface (R = 1). Finally, piles with their bases in Zone C were found to settle less than the surface (R < 1). Therefore for most practical applications reasonable predictions of pile settlement could be made by using the Gaussian curve as a 'greenfield' reference frame.

For the case of the expanding displacement field observed (Standing and Selemetas, 2013), the arrival of the EPBM face beneath a pile located directly above the tunnel induces an axial compressive load of increasing magnitude near the middle of the pile (this correlates well with the large compressive strains measured in the ground at that level). During the passage of the shield beneath the pile there is a significant reduction in the axial load (maximum of 200kN) induced in the pile of increasing magnitude with depth resulting in differential pile settlement relative to the ground. The completion of tail-skin grouting behind the shield induces again a compressive load along the pile resulting in a load distribution that very similar to the original distribution prior to tunnelling. With time the axial load is shown to reduce along the pile to a steady value. The offset piles experienced increases in their base load and negative shaft friction, the magnitude of which depend on the offset distances.

A key messages from the paper is that if there is sufficient reserve shaft capacity (as with the friction piles FC and FO) the pile settlement due to tunnelling can be controlled. However, in the case of end bearing piles, which have already mobilised their shaft friction, the pile has to move more to compensate the loss of end-bearing and the remobilisation of the required capacity.

Acknowledgements

The authors would also like to acknowledge the support provided by Engineering and Physical Science Research Council (EPSRC: GR/S05663/01), Mott MacDonald, the Cambridge European Trust, and the CTRL contract 250 Consortium Joint Venture: Edmund Nuttall/Wayss and Freytag/Kier. Many thanks are also due to several researchers at the Cambridge Geotechnical Group and Imperial College for their assistance in taking some of the field measurements described in this paper. This field study would also not have been made possible without the contributions of Rail Link Engineering and Union Railways (North). The loading frames and control systems were supplied and set up by Precision Measurements and Control of Teeside, UK. Many thanks are also due to Cementation Skanska for their continuous support to this research.

References

Bezuijen, A. and Van der Schrier, J.S. (1994). The influence of a bored tunnel on pile foundations. Proc. of Int. Conf. Centrifuge 94, Singapore (eds C.F. Leung, F.H. Lee & T.S. Tan). Balkema, Rotterdam, pp 681–686.

BS EN 1992-1-1 (2004): Eurocode 2: Design of concrete structures: general rules and rules for buildings. BSI, London, UK.

Chen L.T., Poulos H. G., and Loganathan N. (1999). Pile responses caused by tunnelling. ASCE Journal of Geotechnical and Geoenviromental Engineering, 125(3), pp 207–215.

Coutts D.R. and Wang J. (2000). Monitoring of reinforced concrete piles under horizontal and vertical loads due to tunnelling. Tunnels and Underground Structures (eds J. Zhao, J.N. Shirlaw & R. Krishnan). Balkema, Rotterdam, pp 541–546.

Fellenius, B. H. (1988). Unified design of piles and pile groups. Transportation Research Record 1169. pp 75-83. Transportation Research Board, National Research Council, Washington, D.C., USA.

Fellenius, B.H. (2004). Unified design of piled foundations with emphasis on settlement analysis. Honoring George G. Goble — "Current Practice and Future Trends in Deep Foundations" Geo-Institute Geo-TRANS Conference, Los Angeles, July 27-30, 2004, Edited by J.A. DiMaggio and M.H. Hussein. ASCE Geotechnical Special Publication, GSP 125, pp. 253 - 275.

Fleming, W.G.K. (1992). A new method for single pile settlement prediction and analysis. Géotechnique, Volume 42, Issue 3, September 1992, pp. 411-425.

Fleming W.G.K., Weltman A.J., Randolph M.F. and Elson W.K. (2009). Piling Engineering, 3rd edn. Wiley, New York, USA.

Geilen T. and Taylor G.R. (2001a). The BT building, London Bridge Street. Chapter 34 from Building response to tunnelling: case studies from construction of the Jubilee Line Extension, London, volume 2: case studies (eds J. B. Burland, J. R. Standing, and F. M. Jardine). CIRIA and Thomas Telford, London, pp 683–704.

Geilen T. and Taylor G.R. (2001b). Fielden House, London Bridge Street. Chapter 35 from Building response to tunnelling: case studies from construction of the Jubilee Line Extension, London, volume 2: case studies (eds J. B. Burland, J. R. Standing, and F. M. Jardine). CIRIA and Thomas Telford, London, pp 705–726.

Institution of Civil Engineers (ICE), (2017). Specification for Piling and Embedded Retaining Walls, 3rd Edition, Thomas Telford, London.

Jacobsz S.W., Standing J.R., Mair R.J., Hagiwara T., and Sugiyama T. (2004). Centrifuge modelling of tunnelling near driven piles. Soils and Foundations, 44(1), pp 49–56.

Jacobsz, S.W., Standing, J.R., Mair, R.J., Soga, K., Hagiwara, T. and Sugiyama, T. (2001). Tunnelling effects on driven piles. Proc. Int. Conf. on Response of Buildings to Excavation-Induced Ground Movements, London (ed F.M. Jardine). CIRIA, London, 337-348.

Kaalberg, F.J., Lengkeek, H.J., and Teunissen, E.A.H. (1999). Evaluatie van de meetresultaten van het proefpalenprojek ter plaatse van de tweede Heinenoordtunnel (in Dutch). Adviesbureau Noord/Zuidlijn Technical report no. R981382, Amsterdam.

Loganathan N., Poulos H.G. and Stewart D.P. (2000). Centrifuge model testing of tunnelling-induced ground and pile deformations. Géotechnique, 50(3), pp 283–294.

Mroueh H. and Shahrour I. (2002). Three-dimensional finite element analysis of the interaction between tunnelling and pile foundations. International Journal for numerical and analytical methods in Geomechanics, Vol. 26, no. 3, pp 217–230.

Pang C.H., Yong K.Y. and Chow Y.K. (2006). The response of pile foundations subjected to shield tunnelling. Proc. Int. Conf. on Geotechnical Aspects of Underground Construction in Soft Ground, Amsterdam (eds K.J. Bakker, A. Bezuijen, W. Broere and E.A. Kwast). Taylor and Francis/Balkema, Leiden, Netherlands, pp 737–743.

Price G. and Wardle I. F. (1983). Recent developments in pile-soil instrumentation systems. Proc. Conf. on Field Measurements in Geomechanics, Zurich (ed K. Kovari). Balkema, vol. 1, pp. 2.63 - 2.73.

Selemetas D. (2005). The response of full-scale piles and piled structures to tunnelling. PhD thesis, University of Cambridge.

Selemetas D., Standing J.R., Mair R.J., Sharrocks D.M., Parker F. and Allen R. (2002). The response of a piled structure to tunnelling and jacking. Proc. Int. Conf. on Geotechnical Aspects of Underground Construction in Soft Ground, Toulouse (eds R. Kastner, F. Emeriault, D. Dias & A. Guilloux), Spécifique, Lyon, pp 367-372.

Standing J.R. and Selemetas (2013). Greenfield response to EPBM tunnelling in London Clay. Géotechnique, 63(12), pp 989–1007.

Vermeer P. A. and Bonnier P. G. (1991). Pile settlements due to tunnelling. Proc. 10th European Conference on Soil Mechanics and Foundation Engineering, Florence, (ed Associazione Geotechnica Italiana). A.A. Balkema, Rotterdam, Netherlands, Vol. 2, pp 869–872.

Tables

Table 1. Summary of pile load-displacement response during working pile test.

Pile FO		Pile FC		Pile BO		Pile BC	
P (kN)	Sp (mm)	P (kN)	Sp (mm)	P (kN)	Sp (mm)	P (kN)	Sp (mm)
0	0	0	0	0	0	0	0
40	-0.01	41	-0.03	150	-0.29	151	-0.38
81	-0.08	81	-0.06	258	-0.84	251	-0.84
120	-0.24	121	-0.24	352	-1.46	351	-1.41
160	-0.34	161	-0.34	453	-2.38	451	-2.06
200	-0.48	200	-0.48	553	-3.35	550	-2.78
240	-0.66	241	-0.65	652	-4.60	651	-3.80

Table 2. Summary of CemSet parameters used to back-analyse pile test response (for all piles shaft flexibility factors Ms = 0.0015 and friction centroid = 0.45).

Pile Ref	Shaft diameter (mm)	Base diameter (mm)	Shaft free length (m)	Shaft friction length (m)	USF (kN)	UEB (kN)	E_b (kPa)
FO	480	500	4.5	8.5	960	140	20000
FC	480	500	4.5	8.5	960	140	20000
BO	480	500	4.5	4.0	400	1963	150000
BC	480	500	4.5	4.0	430	1963	120000

Notes: USF = Ultimate Shaft Friction

UEB = Ultimate End Bearing

E_b = Soil modulus at pile base

List of figures

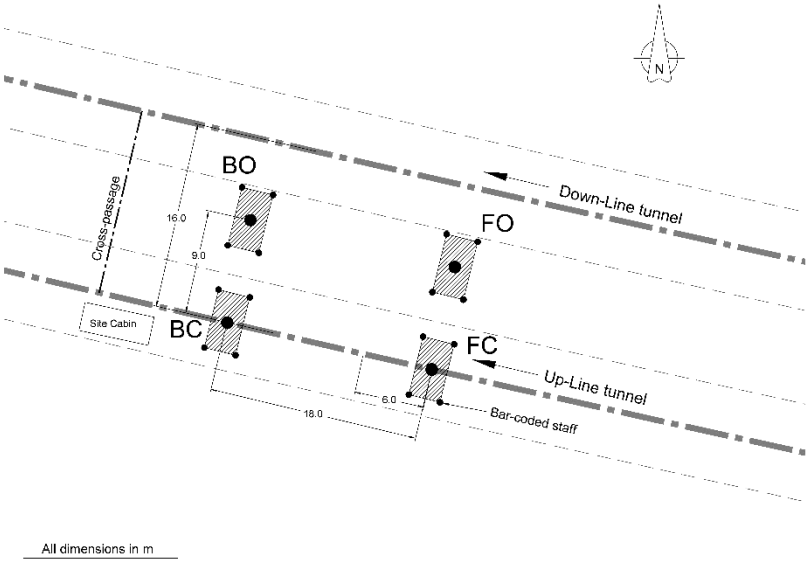
N
BO
FO
BC
FC
Down-Line tunnel
Up-Line tunnel
Cross-passage
Site Cabin
16.0
9.0
6.0
18.0
Bar-coded staff
All dimensions in m

a)

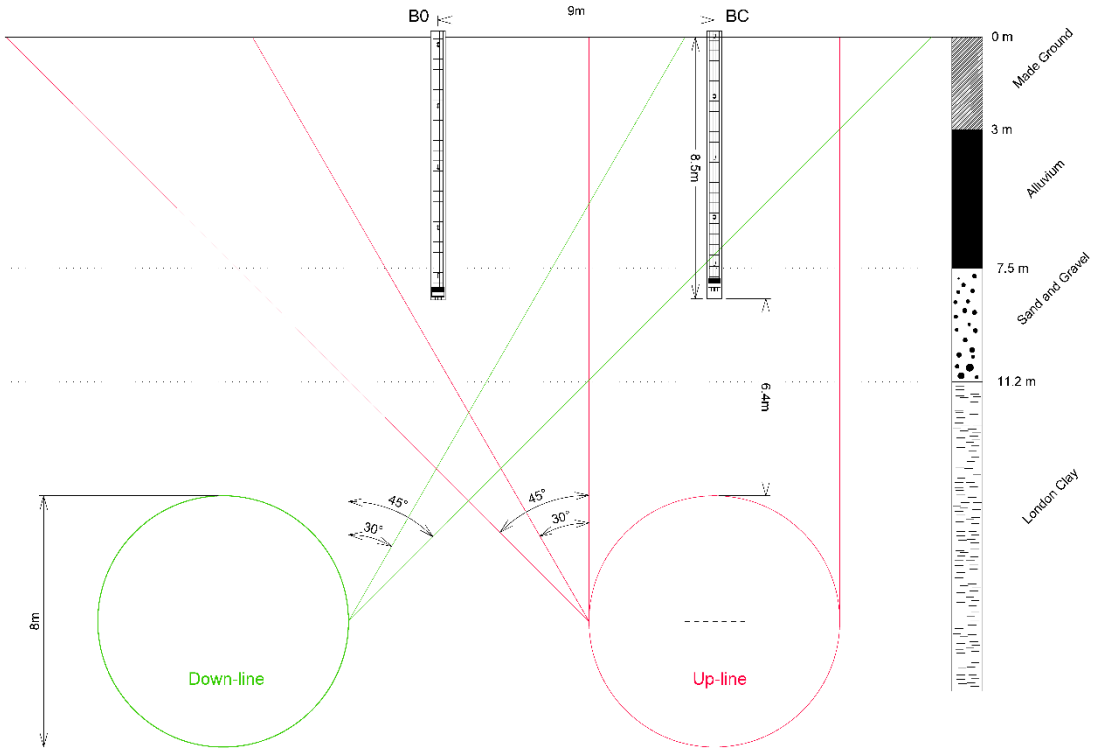
B0
9m
BC
8.5m
6.4m
0 m
Made Ground
3 m
Alluvium
7.5 m
Sand and Gravel
11.2 m
London Clay
45°
30°
45°
30°
8m
Down-line
Up-line

b)

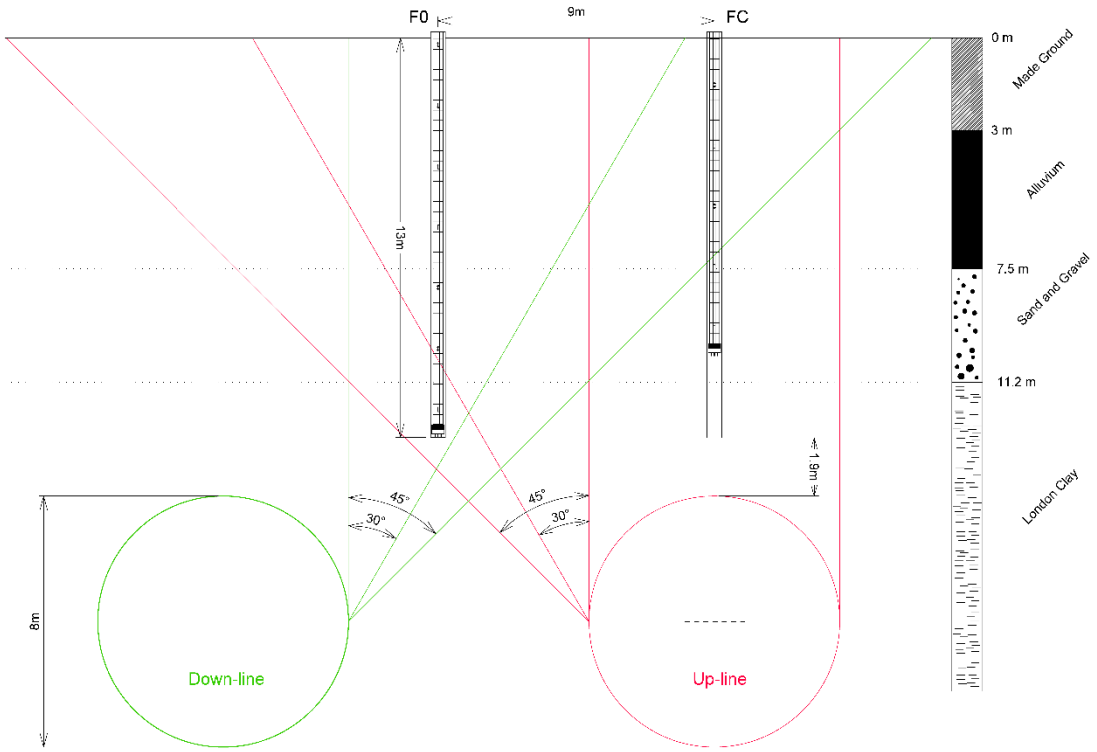

c)

Figure 1. a) Plan view and b) cross-sections of instrumented piles with reference to twin tunnel alignment.

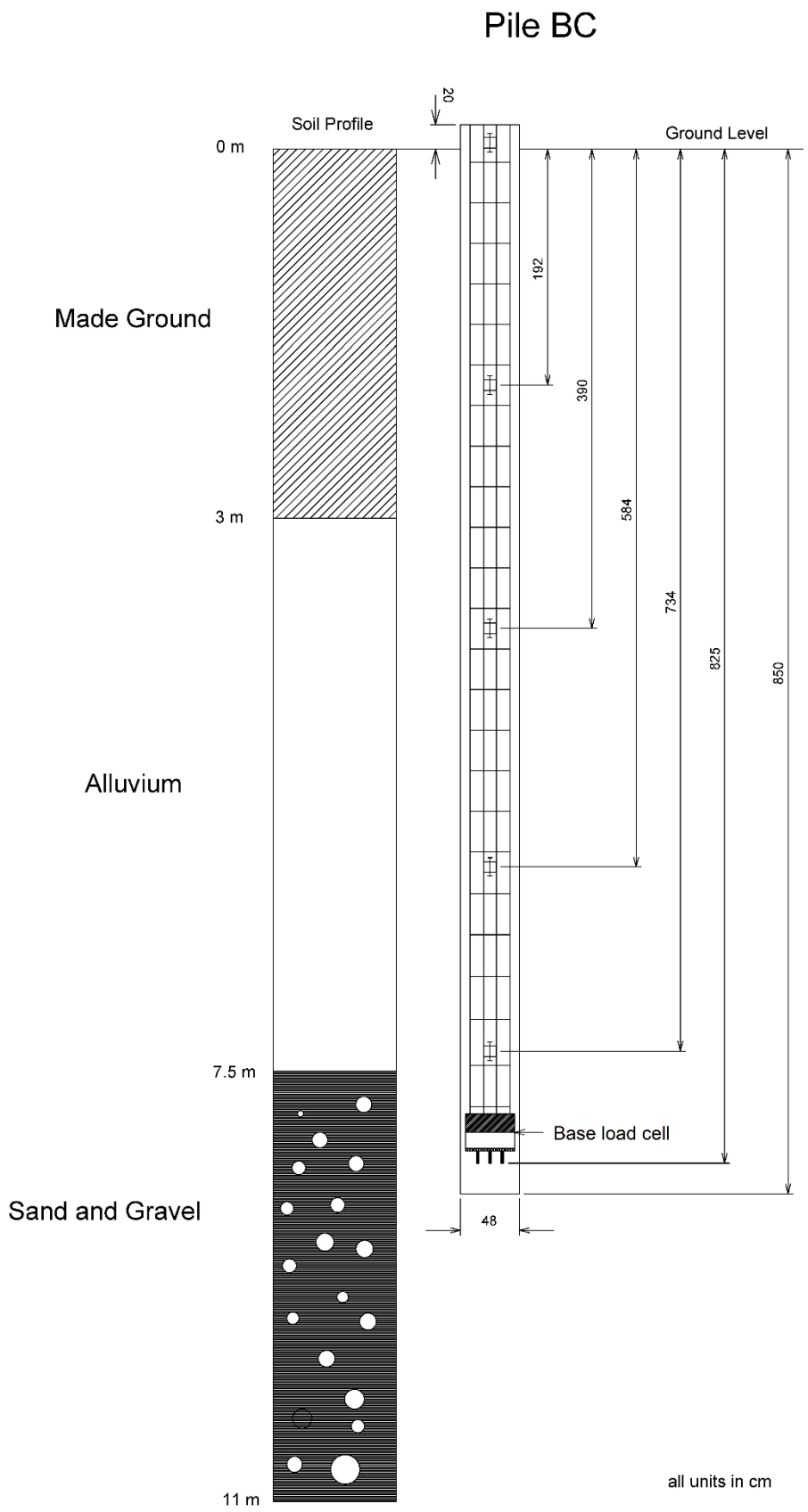
Pile BC
Soil Profile
Ground Level
0 m
3 m
7.5 m
11 m
Made Ground
Alluvium
Sand and Gravel
20
192
390
584
734
825
850
Base load cell
48
all units in cm

a)

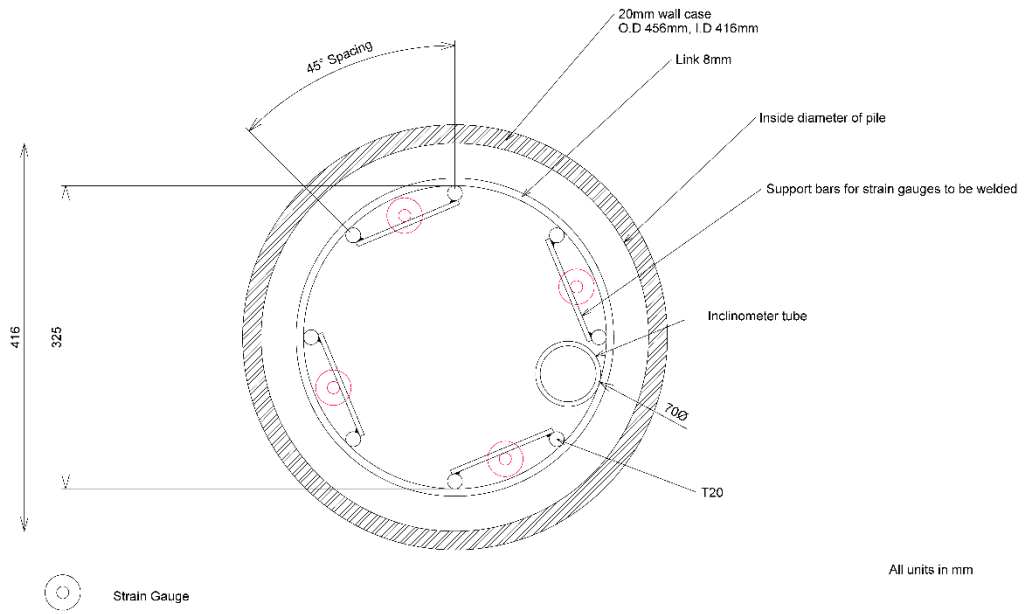
20mm wall case
O.D 456mm, I.D 416mm
45° Spacing
Link 8mm
Inside diameter of pile
Support bars for strain gauges to be welded
Inclinometer tube
700
T20
416
325
All units in mm
Strain Gauge

b)

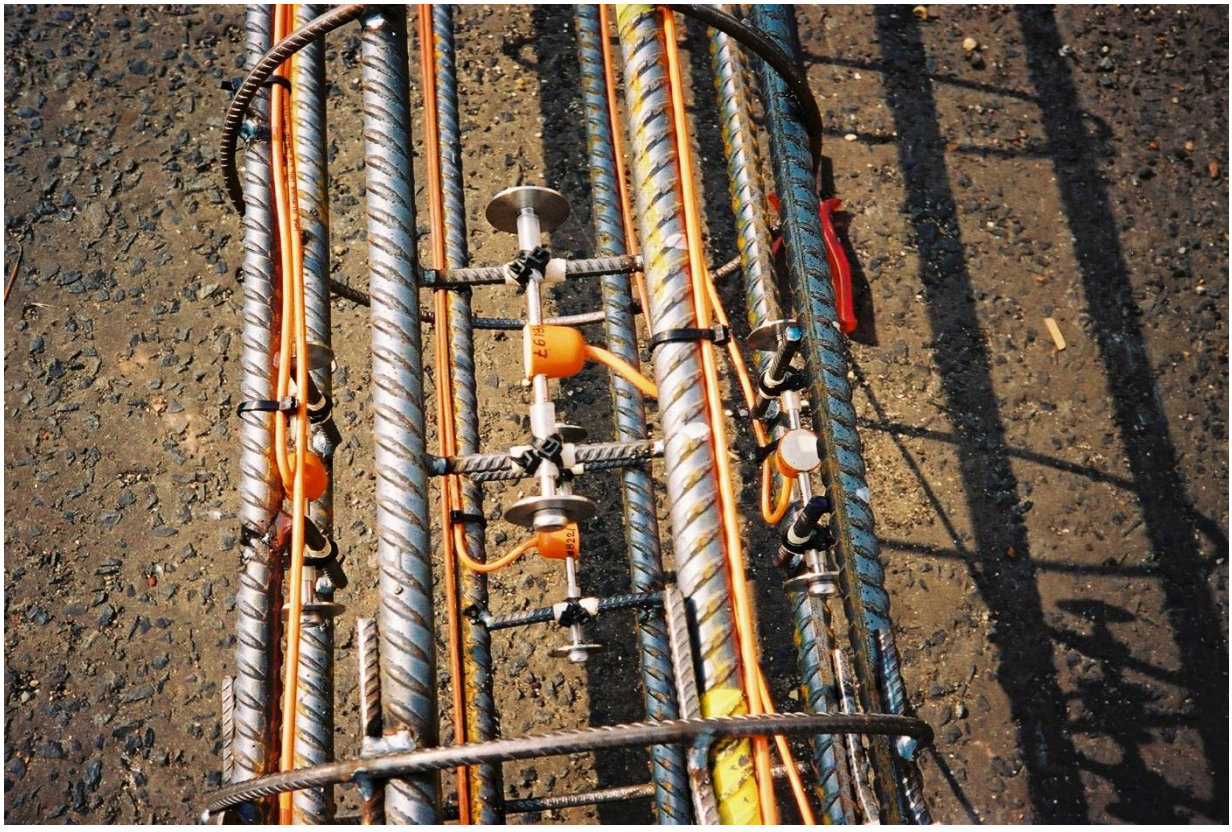

c)

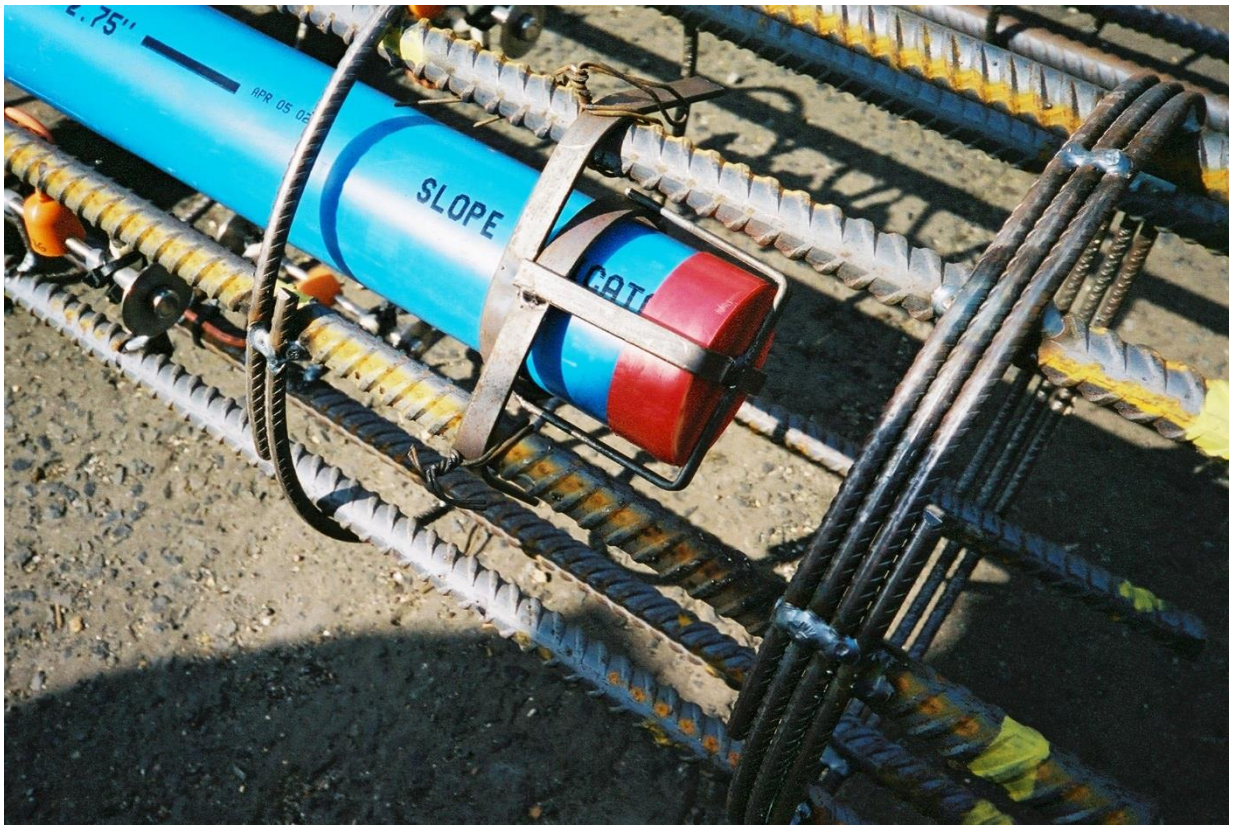

d)

Figure 2. Details of instrumentation along piles: schematics of typical arrangements of strain gauges (a) along length of pile BC and (b) across a pile section; photographs showing attachments to pile reinforcement of (c) strain gauges and (d) inclinometer tubes.

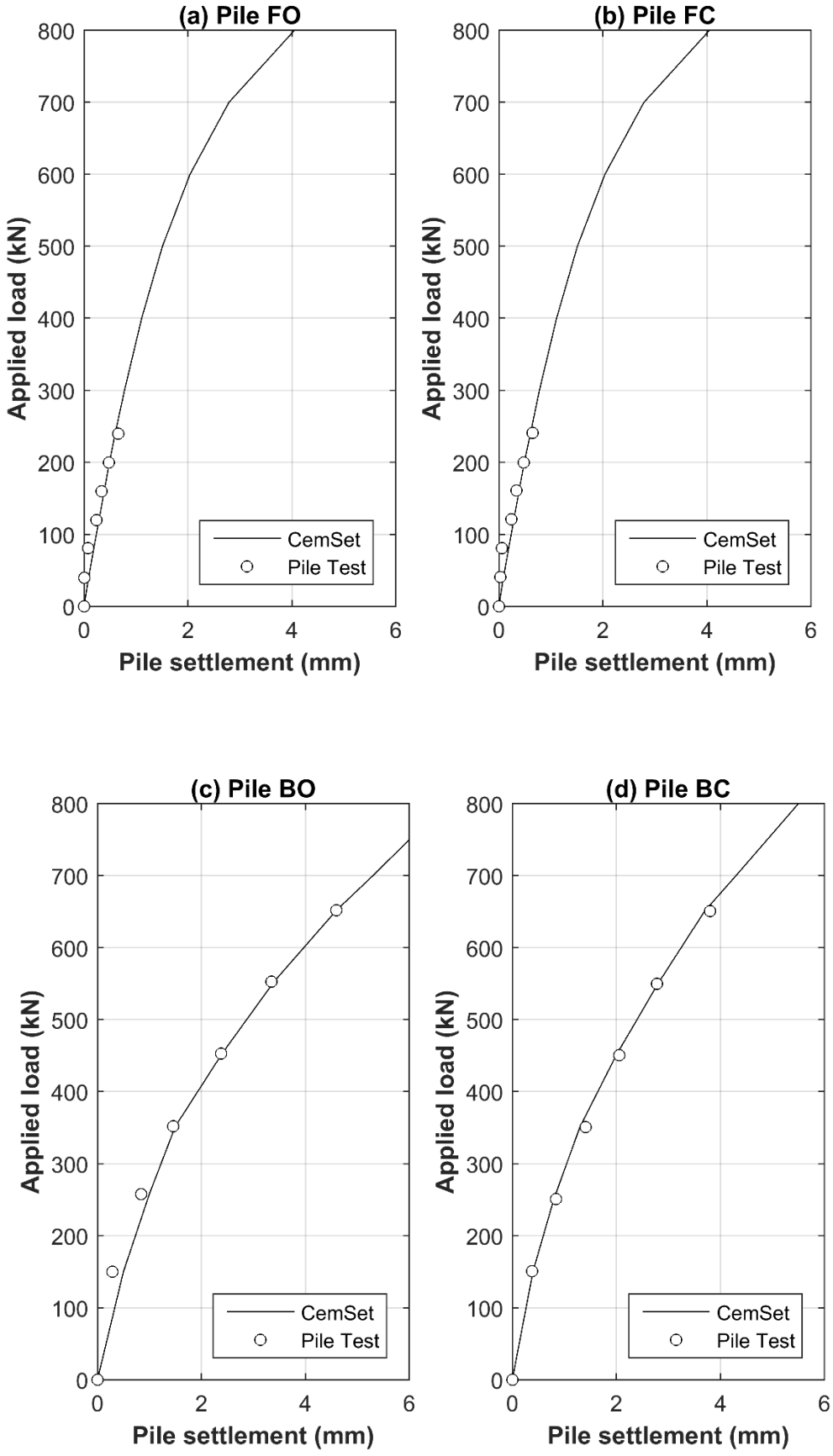

Figure 3. Pile load-test settlement results compared with CemSet model predictions.

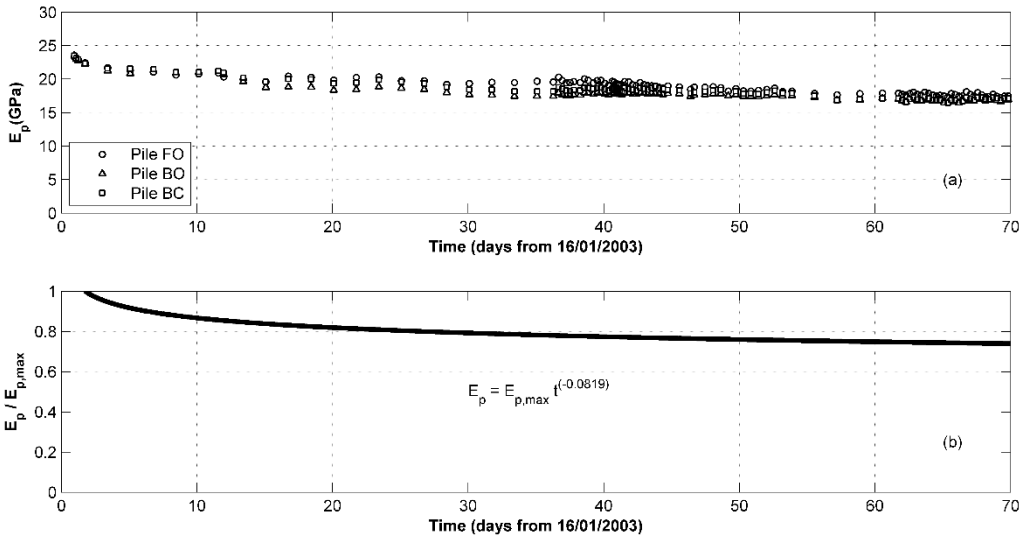

Figure 4. Relationship of apparent pile stiffness degradation with time (a) back-calculated values from measurements, (b) normalized best-fit curve.

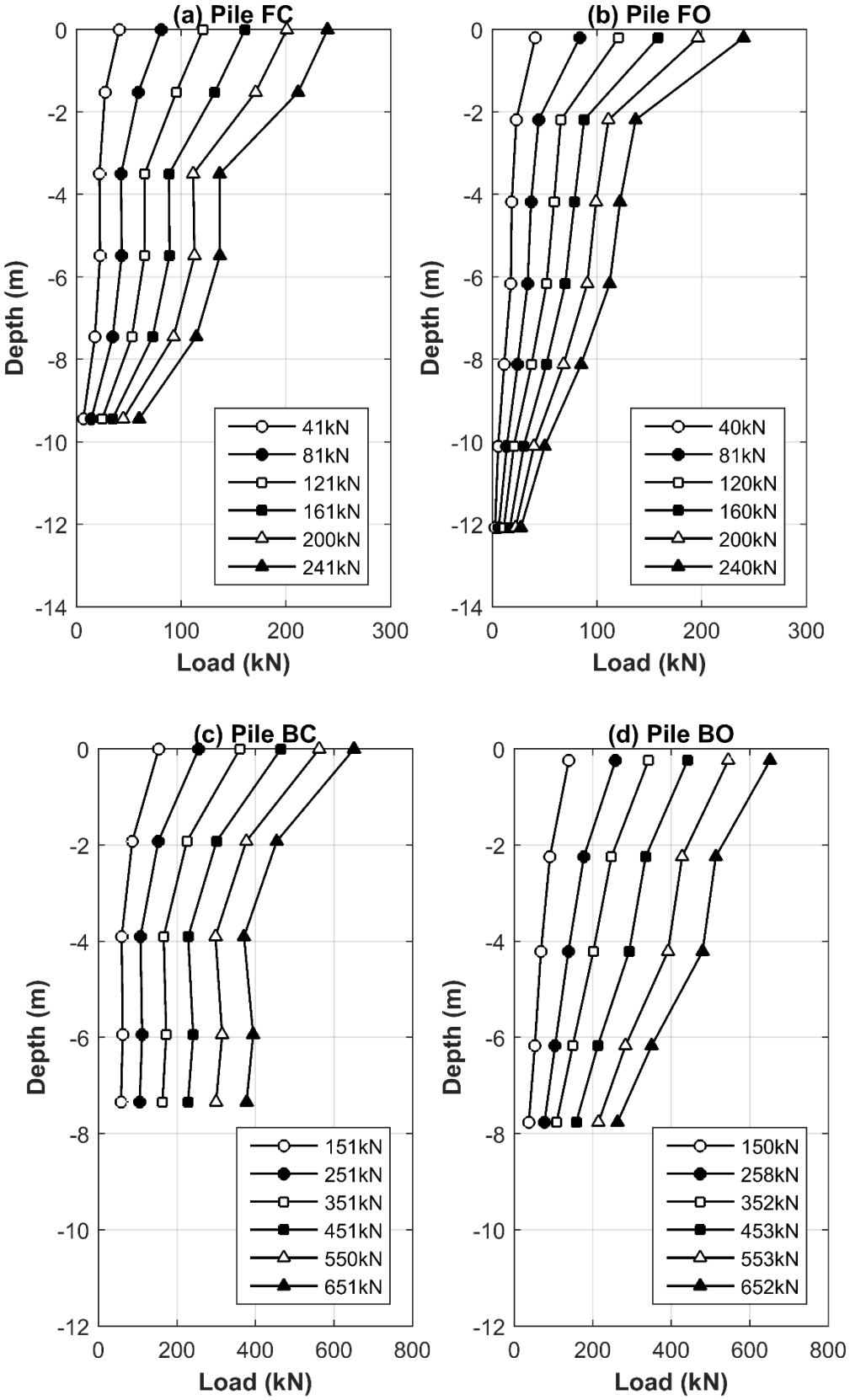

Figure 5. Pile load transfer curves during pile loading (legend gives applied head loads).

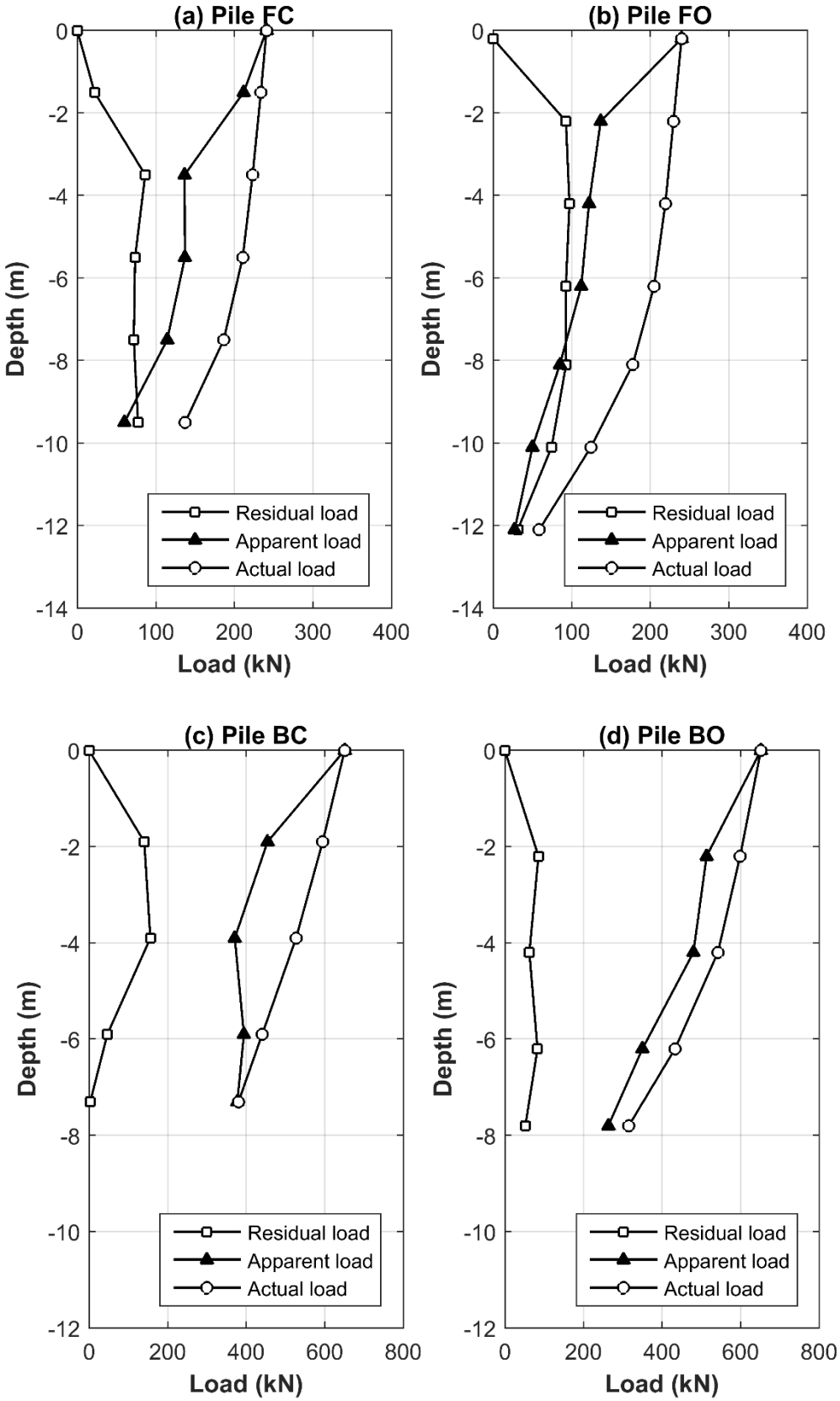

Figure 6. Pile load distribution curves including residual load effects at the end of pile loading (16.01.2003).

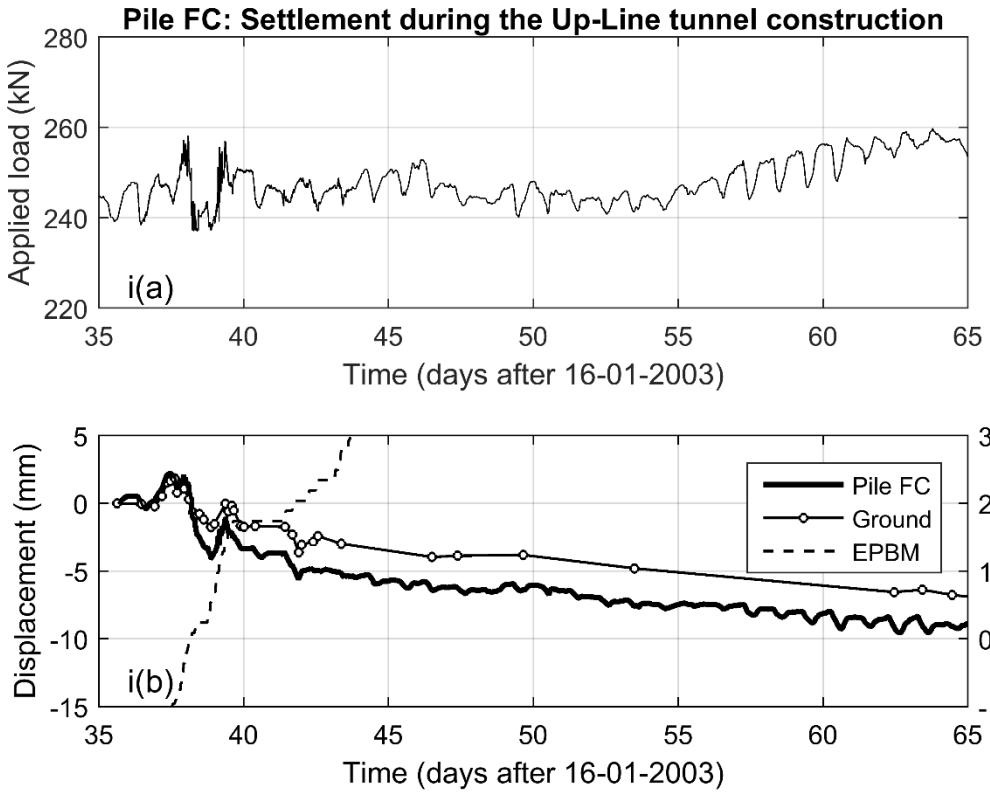
Pile FC: Settlement during the Up-Line tunnel construction
Applied load (kN)
280
260
240
220
i(a)
35
40
45
50
55
60
65
Time (days after 16-01-2003)
Displacement (mm)
5
0
-5
-10
-15
Distance from face (m)
30
20
10
0
-10
Pile FC
Ground
EPBM
i(b)
Time (days after 16-01-2003)

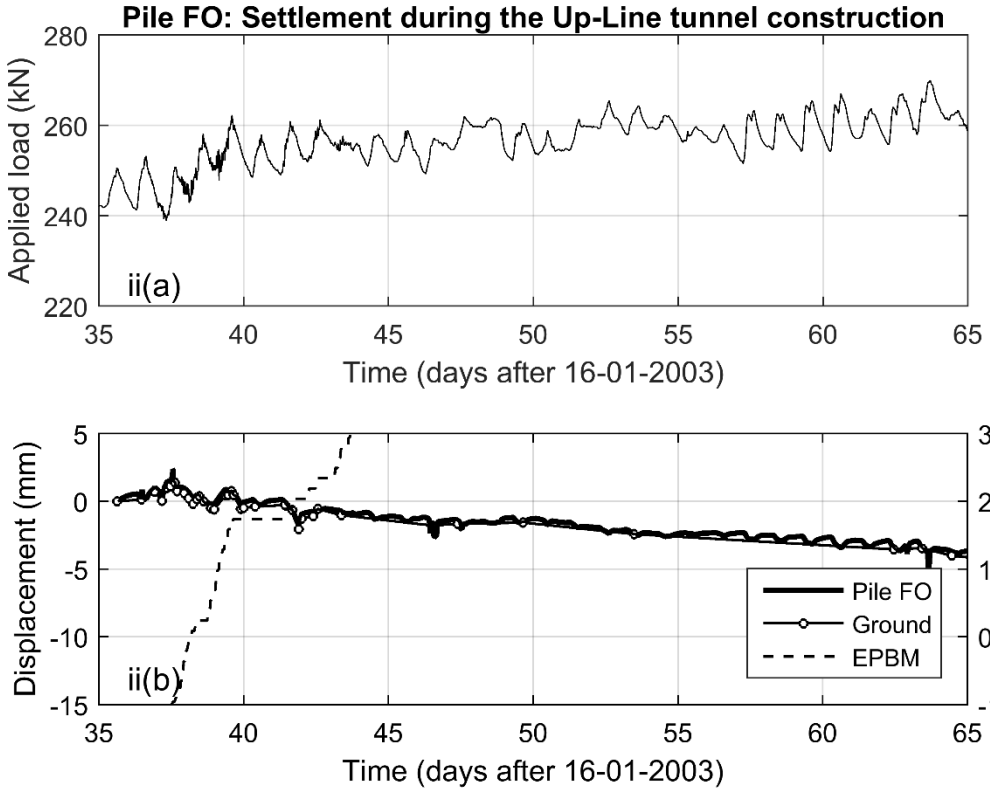
Pile FO: Settlement during the Up-Line tunnel construction
Applied load (kN)
280
260
240
220
ii(a)
35
40
45
50
55
60
65
Time (days after 16-01-2003)
Displacement (mm)
5
0
-5
-10
-15
Distance from face (m)
30
20
10
0
-10
Pile FO
Ground
EPBM
ii(b)
Time (days after 16-01-2003)

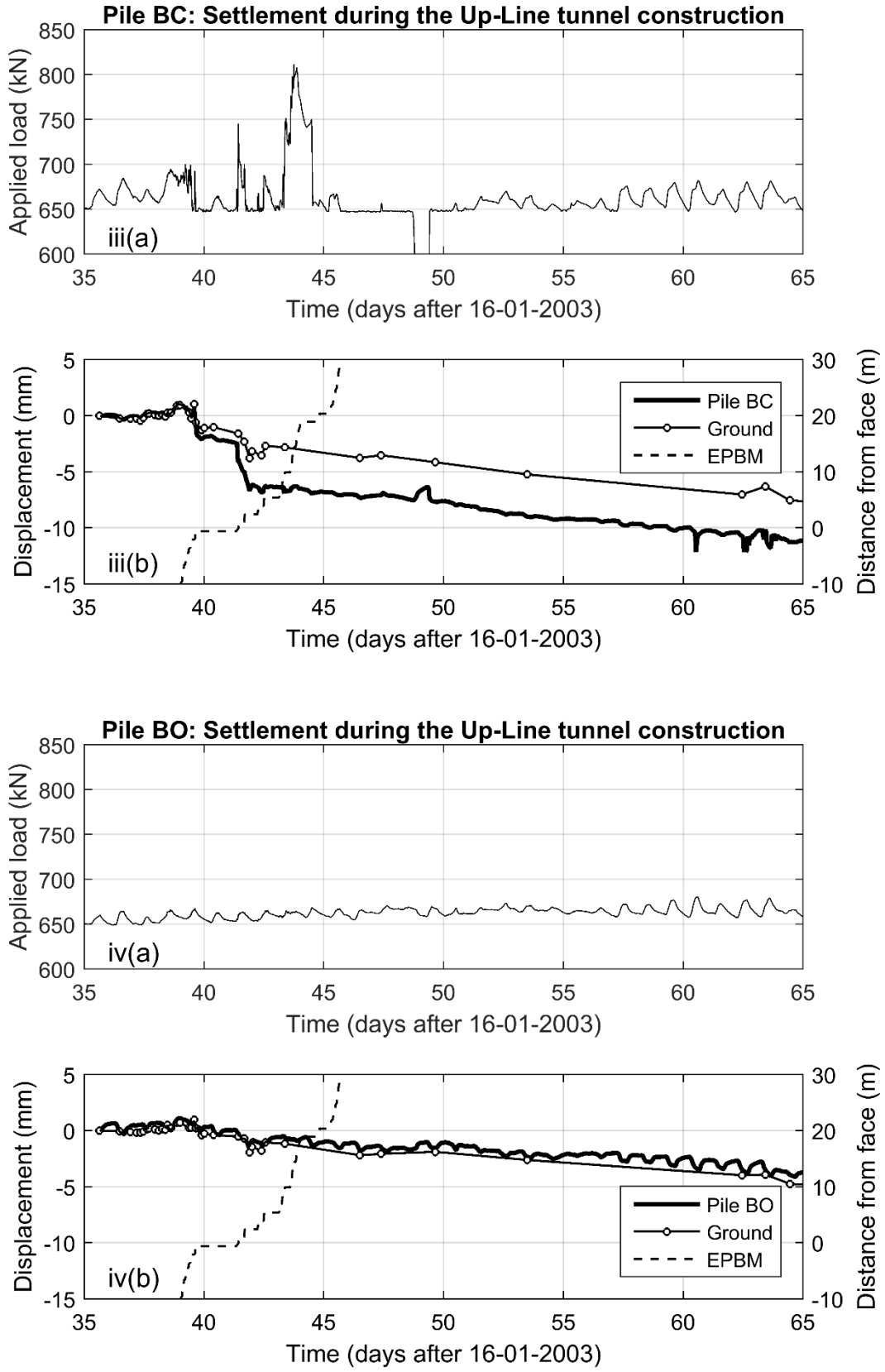

Figure 7. Development of (a) applied pile load and (b) pile head displacement compared with the surrounding ground displacement during passage of the Up-Line TBM for piles (i) FC; (ii) FO; (iii) BC and (iv) BO.

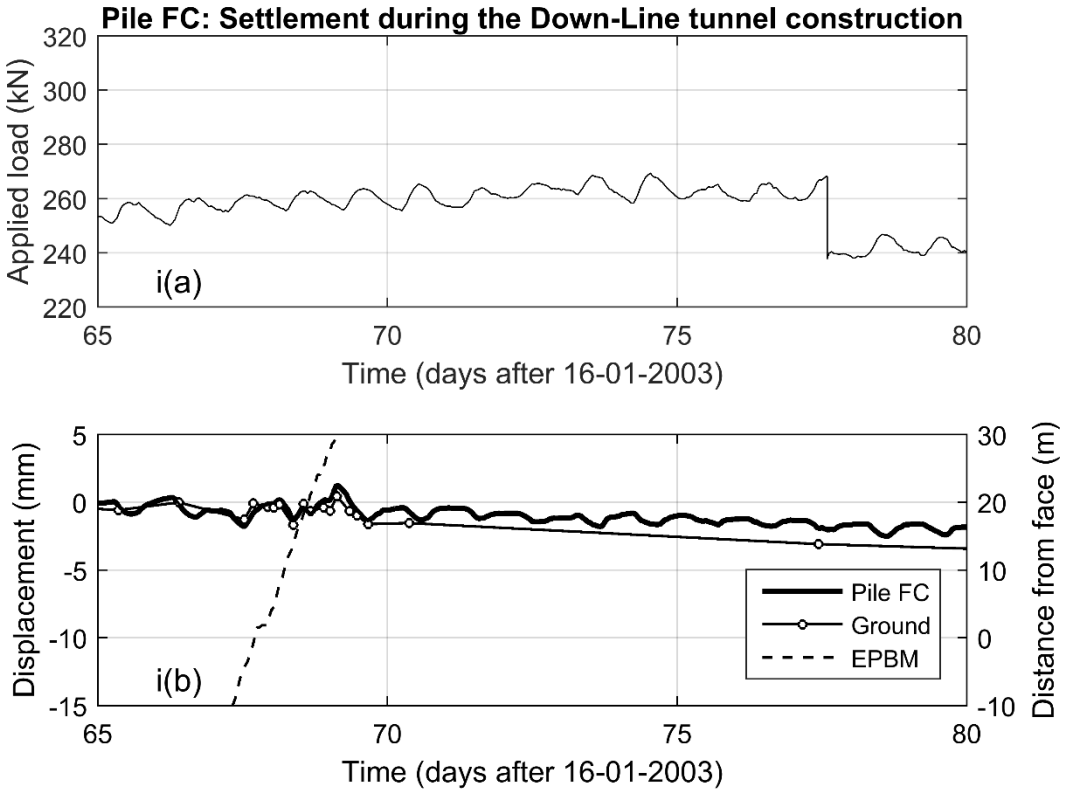
Pile FC: Settlement during the Down-Line tunnel construction
Applied load (kN)
320
300
280
260
240
220
i(a)
65
70
75
80
Time (days after 16-01-2003)
Displacement (mm)
5
0
-5
-10
-15
30
20
10
0
-10
Distance from face (m)
Pile FC
Ground
EPBM
i(b)
65
70
75
80
Time (days after 16-01-2003)

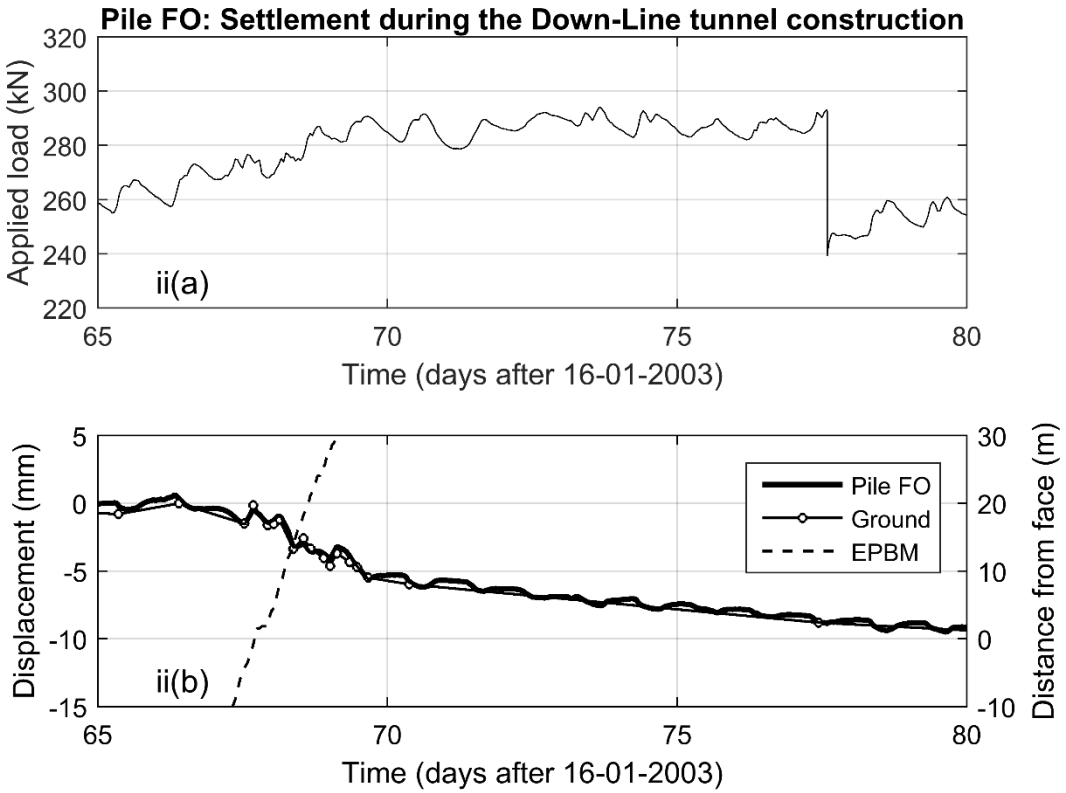
Pile FO: Settlement during the Down-Line tunnel construction
Applied load (kN)
320
300
280
260
240
220
ii(a)
65
70
75
80
Time (days after 16-01-2003)
Displacement (mm)
5
0
-5
-10
-15
30
20
10
0
-10
Distance from face (m)
Pile FO
Ground
EPBM
ii(b)
65
70
75
80
Time (days after 16-01-2003)

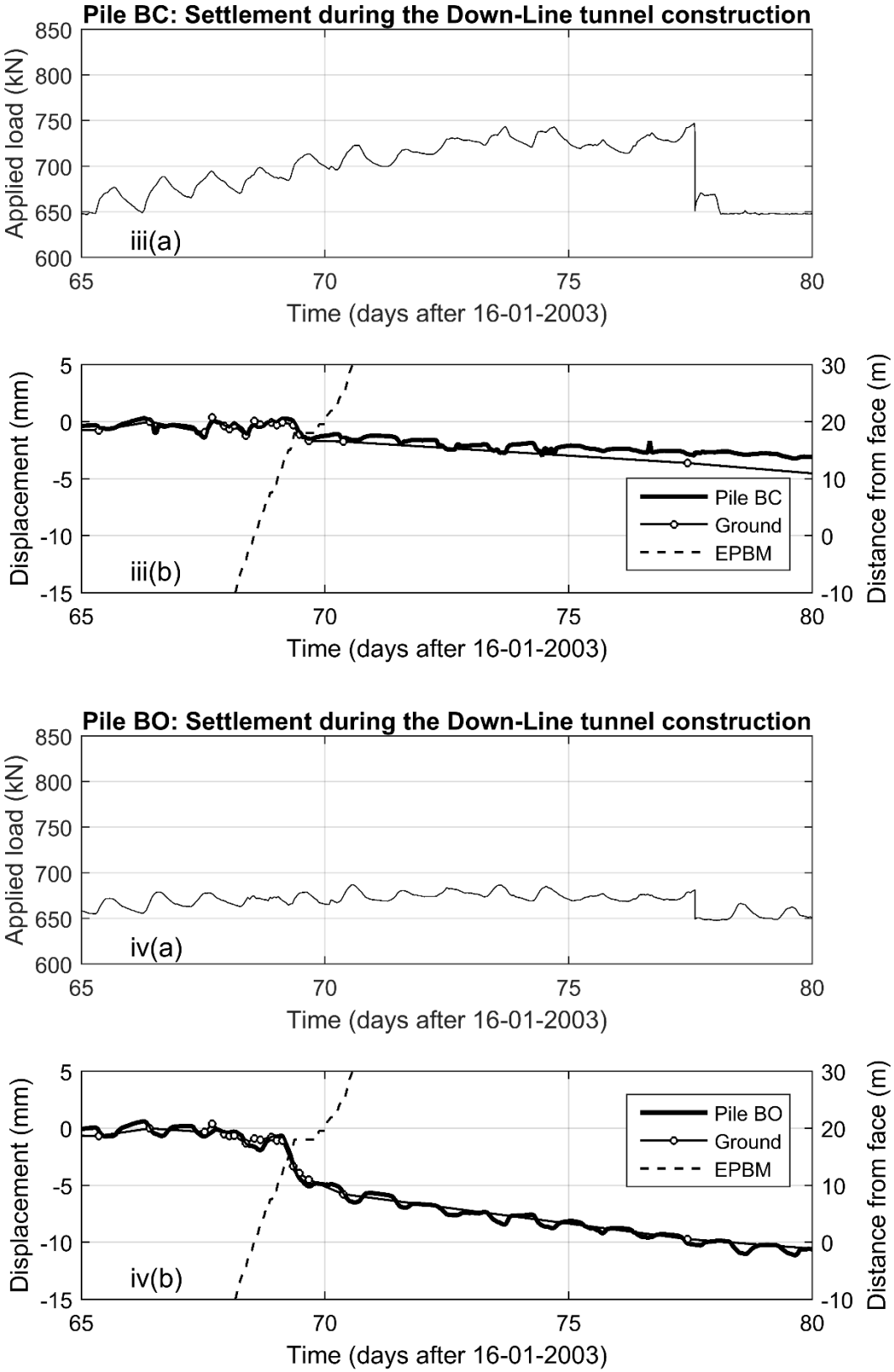

Figure 8. Development of (a) applied pile load and (b) pile head displacement compared with the surrounding ground displacement during passage of the Down-Line TBM for piles (i) FC; (ii) FO; (iii) BC and (iv) BO.

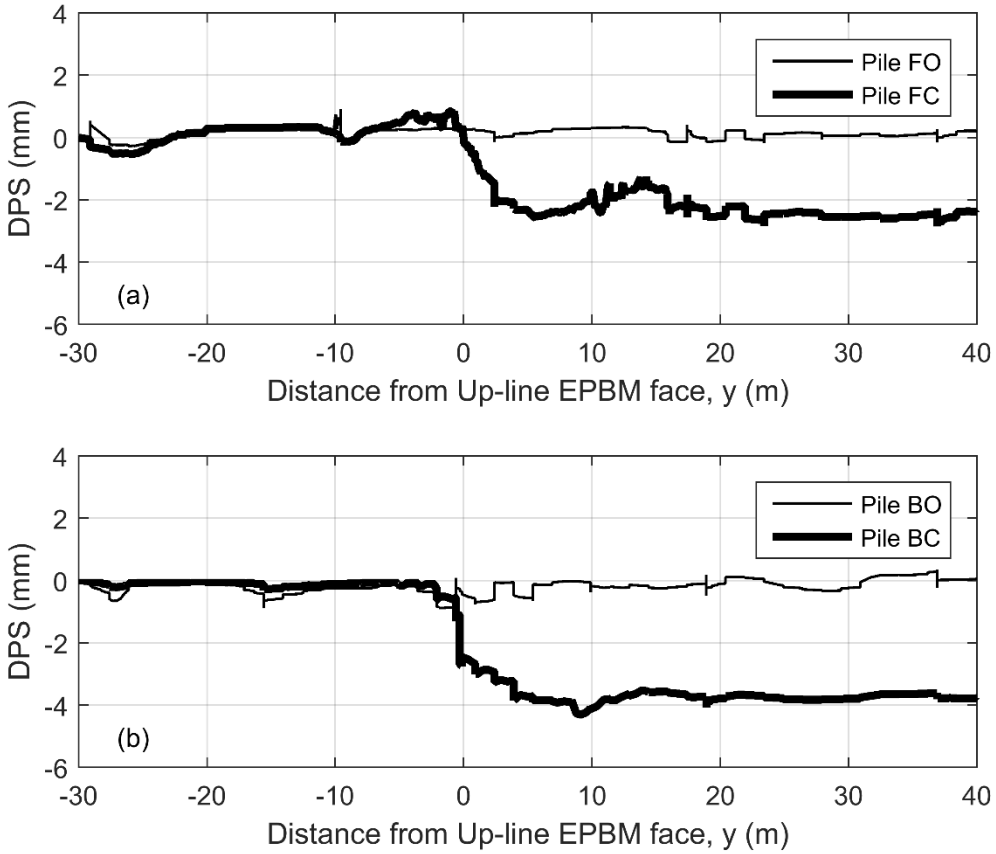

Figure 9. Development of differential pile displacements during approach and passage of Up-Line EPBM TBM drive different phases of earth pressure balance machine operation for (a) piles FC and FO and (b) piles BC and BO (DPS = Differential Pile Settlement; DPH = Differential Pile Heave).

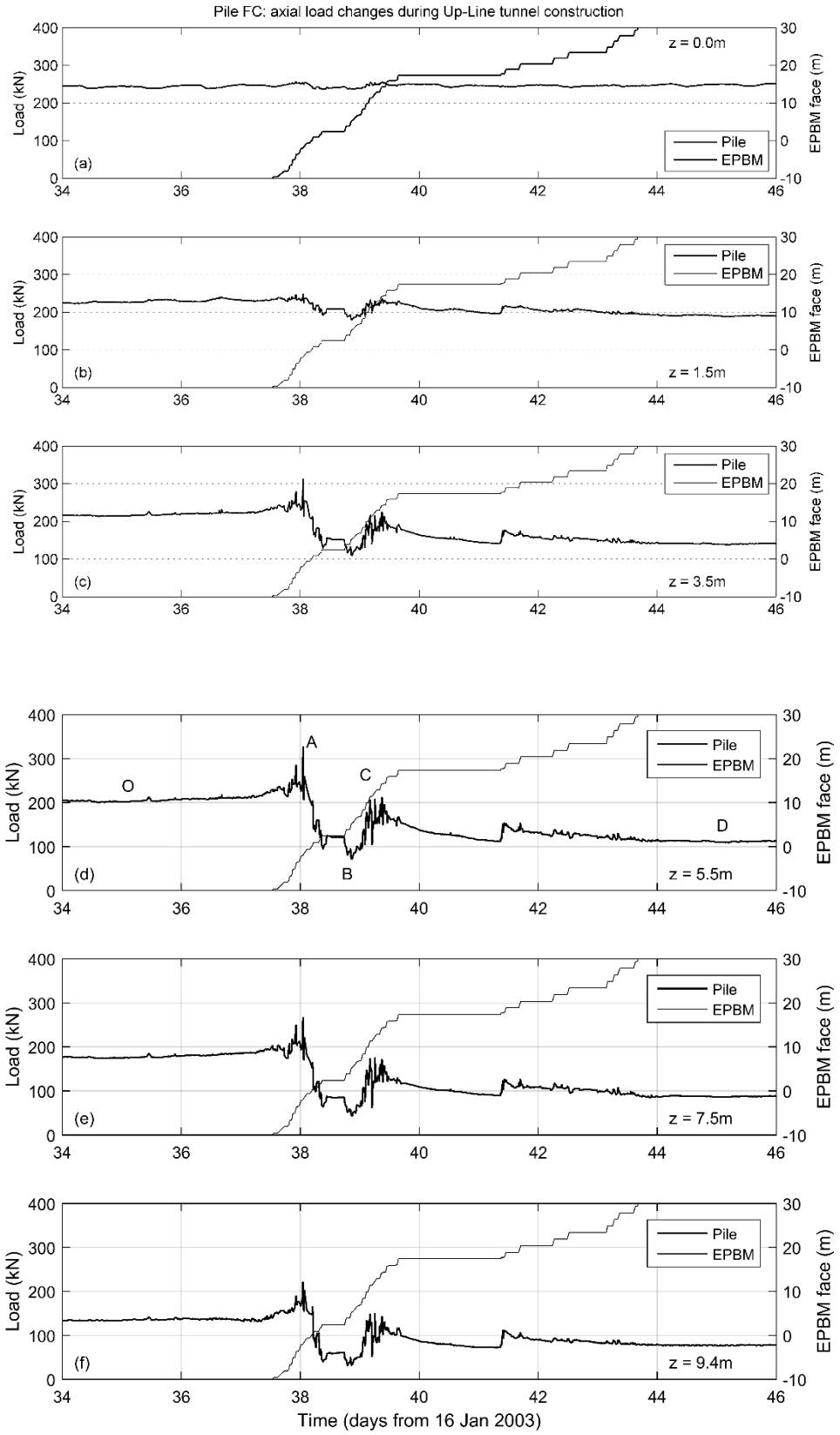

Figure 10. Changes in the axial load distribution along the length of pile FC due to the Up-Line tunnel construction (key changes: point O – initial load distribution prior to tunnelling; point A – load distribution when the EPBM face is beneath the pile; point B – load distribution when the whole tunnelling shield has passed beneath the pile; point C – end of tail-grouting behind the shield; point D – final load distribution after tunnelling).

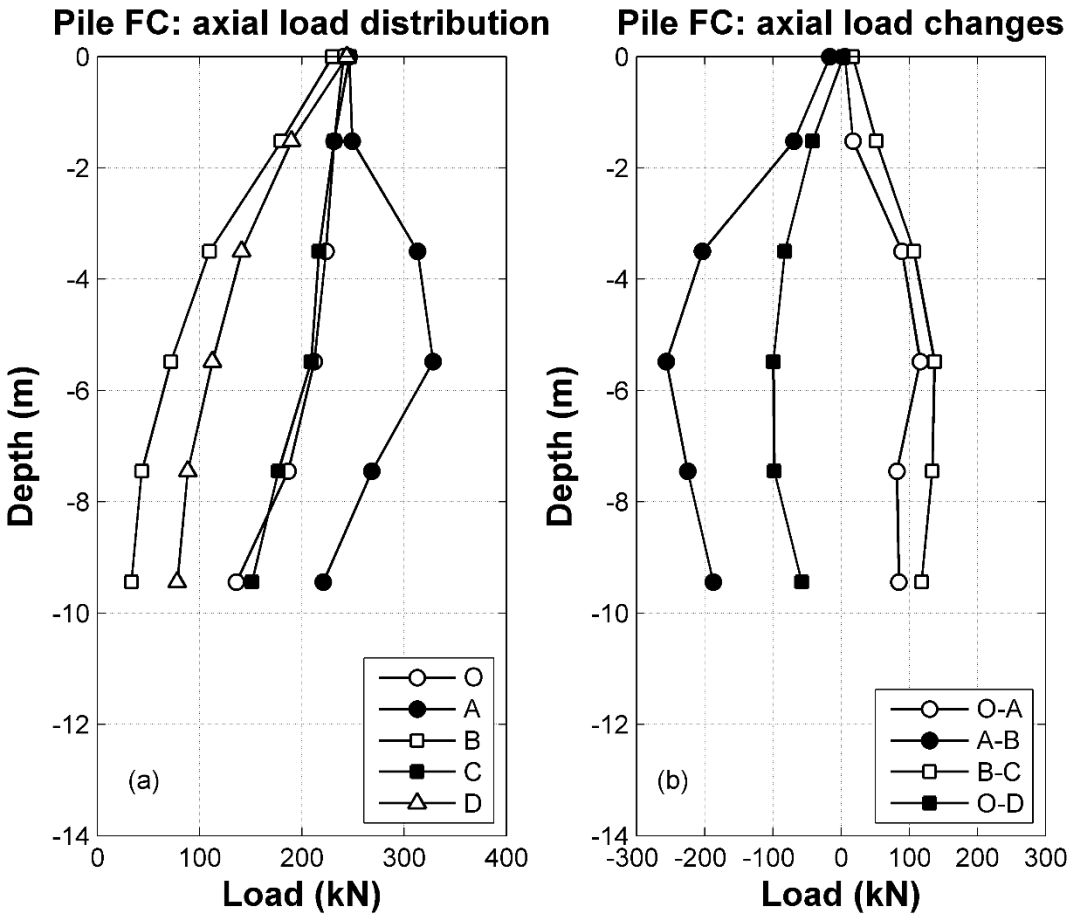

Figure 11. (a) Axial load distributions in pile FC for key events during construction of Up-Line tunnel, (b) key changes in the axial load distribution along pile FC during the Up-Line tunnel construction (as given in Figure 10: point O – initial load distribution prior to tunnelling; point A – load distribution when the EPBM face is beneath the pile; point B – load distribution when the whole tunnelling shield has passed beneath the pile; point C – end of tail-grouting behind the shield; point D – final load distribution after tunnelling).

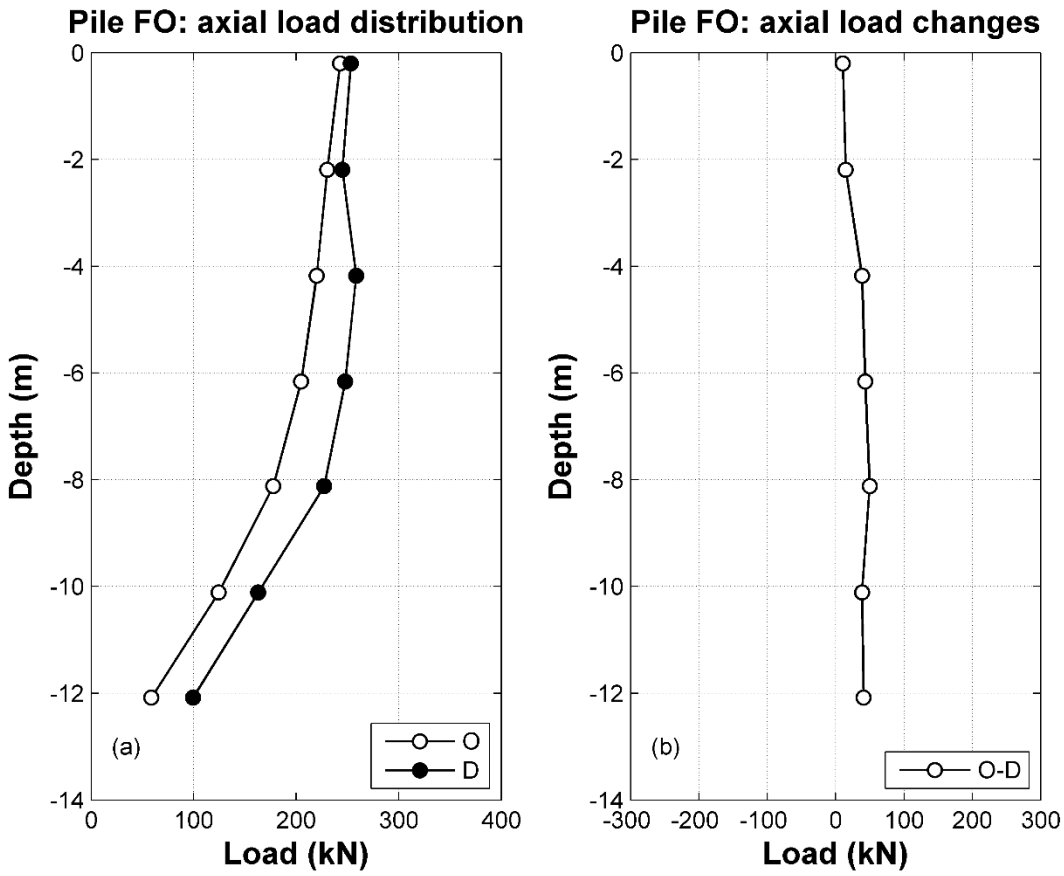

Figure 12. (a) Axial load distributions in pile FO prior to and following construction of Up-Line tunnel, (b) change in the axial load distribution along pile FO during the Up-Line tunnel construction (point O represents the initial load distribution prior to tunnelling and D denotes the final load distribution after tunnelling).

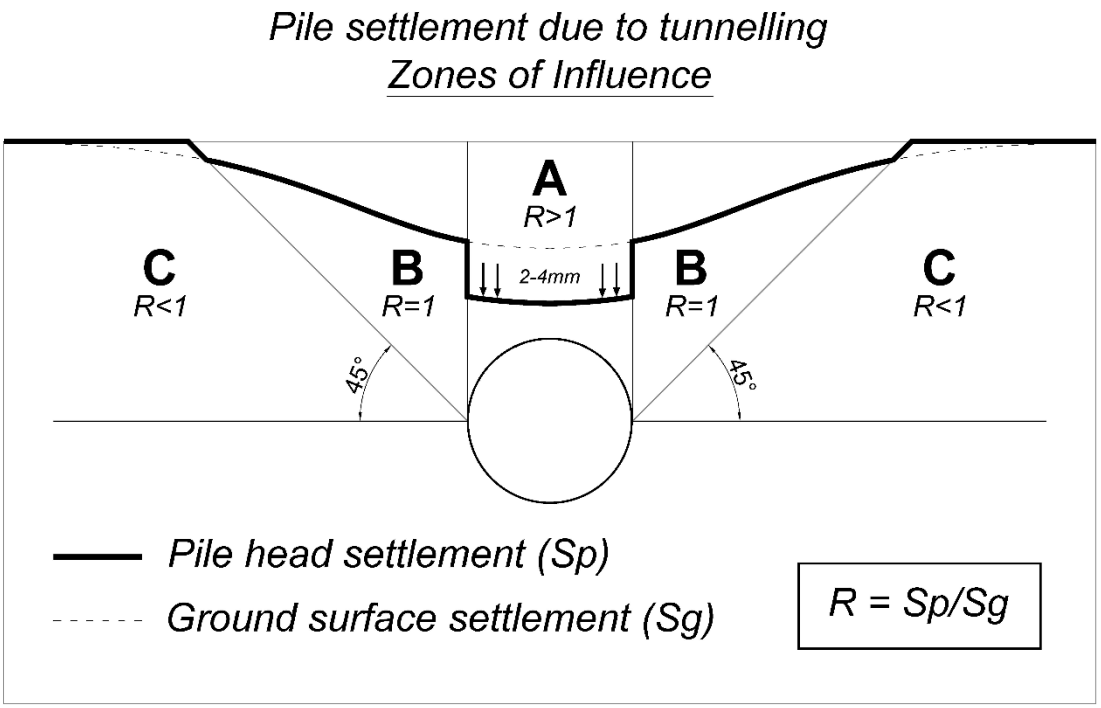

Figure 13. Zones of influence around an Earth Pressure Balance Machine showing pile settlement relative to ground surface settlement.

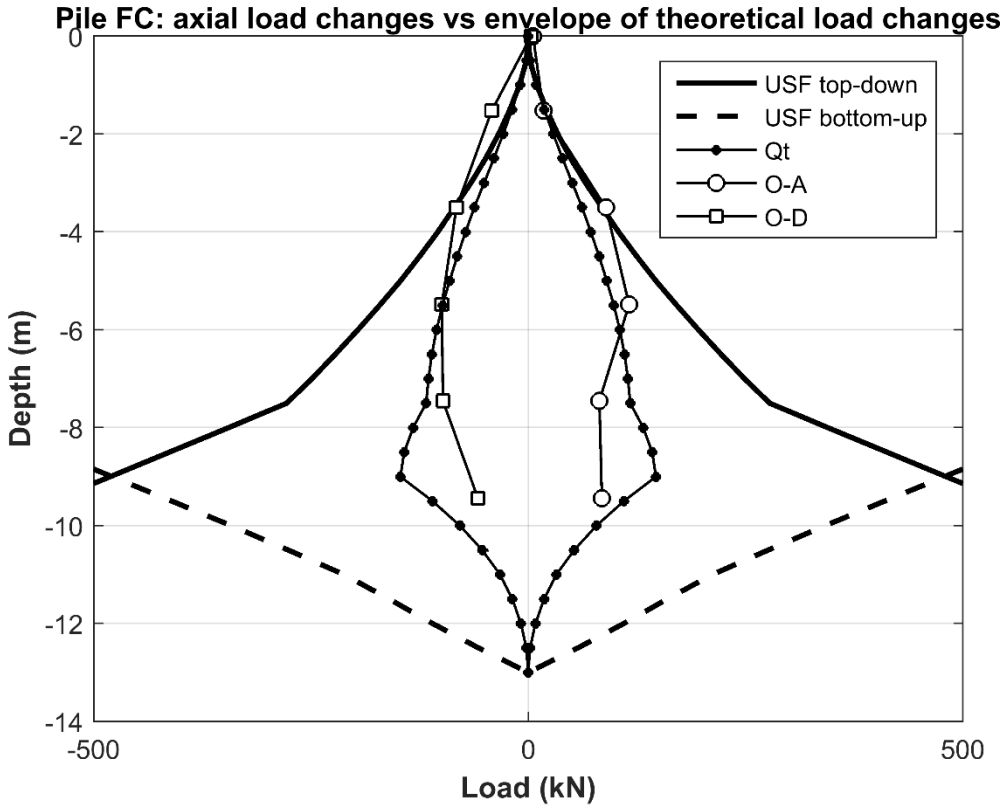

Figure 14. Tunnelling-induced load changes in a pile based compared versus envelope of theoretical load changes based on shaft friction back-calculated during pile test.